Bulletin 73

Vertical Electrical Resistivity Soundings To Locate Ground Water Resources: A Feasibility Study

Mohamed A. Sabet

Bulletin 73
November 1975

Vertical Electrical Resistivity Soundings To Locate Ground Water Resources: A Feasibility Study

Mohamed A. Sabet
Department of Geophysical Sciences
Old Dominion University
Norfolk, Virginia 23508

The research on which this publication is based was supported by the Virginia Polytechnic Institute and State University, Research Division, Blacksburg, Virginia.

VPI-WRRC-BULL 73

A publication of
Virginia Water Resources Research Center
Virginia Polytechnic Institute and State University
Blacksburg, Virginia 24061

TABLE OF CONTENTS

LIST OF FIGURES

ABSTRACT

This report discusses the occurrence of ground water in the Coastal Plain region of southeastern Virginia and northeastern North Carolina, as indicated by the results of 45 vertical resistivity soundings (VES). These soundings were taken with the Schlumberger array with a maximum separation of 8,000 feet between the current electrodes. VES data was interpreted through an automatic computer interpretation program, and by the curve-matching method.

The results reported here suggest that, in the area west of the town of Suffolk, the depth to the basement complex can be determined with reasonable confidence. Eastwards from Suffolk, an "electric basement" of high resistivity was detected at depths which usually exceeded 1,000 feet. The correlation between some VES interpretations and resistivity logs of wells in their vicinities reveals high degrees of similarities.

ACKNOWLEDGEMENTS

The work upon which this report is based was supported by funds provided by the Virginia Water Resources Research Center. The computer programs were provided by Dr. A. A. R. Zohdy of the U.S. Geological Survey in Denver, Colorado, with whom the author had numerous sessions of beneficial discussions. The computer time was donated by the Old Dominion University, and Dr. William J. Hanna of the Department of Geophysical Sciences at Old Dominion reviewed the typescript.

Special acknowledgement is accorded the following, who generously gave their time to a critical review of the manuscript: I. Wendell Marine, Savannah River Laboratory, E. I. du Pont de Nemours & Company, Aiken, South Carolina; and Dr. Adel A. R. Zohdy, U.S. Geological Survey, Denver, Colorado. Acknowledgement is also made to Katherine Miller Kurtz, Victoria Esarey, and Charlotte R. Hungate, who did the typesetting for this Bulletin.

INTRODUCTION

Electrical exploration methods may be subdivided into two main groups. One group is concerned with measurement of resistivity, or conductivity, of rocks; the other group is concerned with measurement of their capacitance. The galvanic, induction, magneto-telluric, and telluric methods belong to the first group, and the induced polarization methods belong to the second group. All resistivity methods can be applied for studying variations of resistivity with depth (depth sounding methods) or for studying lateral changes in resistivity (horizontal profiling methods). The vertical electrical resistivity sounding methods (VES) are depth sounding galvanic methods.

The electrical resistivity of rock is a property which depends on lithology and fluid content. The resistivity of coarse-grained, well-consolidated sandstone saturated with fresh water is higher than that of unconsolidated silt of the same porosity, saturated with the same water. Also, the resistivities of identical porous rock samples vary considerably according to the salinity of the saturating water. The higher the salinity of the water, the lower the resistivity of the rock. Thus, it is quite possible for two different types of rock, such as shale and sandstone, to be of essentially the same resistivity when the sandstone is saturated with saline water and the shale with fresh water. For this reason, the number and thicknesses of the geoelectric units as determined from VES measurements at a locality may not necessarily be the same as the geological ones. In this respect, geoelectric units define parastratigraphic units (Krumbein and Sloss, 1963, p. 333) whose boundaries may be discordant with the stratigraphic boundaries.

The ultimate objective of a VES at some locality is to obtain a true resistivity log similar to, for example, the induction log of a well at the locality, without actually drilling the well. However, because of inherent limitations (which will be discussed briefly), the resolution of the VES methods is not as high as that of the induction log. Nonetheless, the VES methods remain as the most inexpensive methods of subsurface exploration. They surpass the more expensive seismic method in one major respect. The seismic signal associated with a sandstone body would be the same whether its pores are saturated with fresh or with brackish water. On the other hand, its resistivity varies according to small changes in water salinity. This property together with the low cost make the VES methods very suitable for groundwater exploration.

The VES methods were introduced by Schlumberger in 1934. Since then, a wide variety of VES arrays were developed (Keller and Frischknecht, 1966, pp. 90-196), but the Schlumberger array remained as the best array for depth sounding. However, application of the VES techniques were, until recently, limited to shallow investigations, mainly because electronic measuring devices of sufficient sensitivity were not available except in bulky forms, and partly because deeper penetration would have meant a wider variety of resistivity layers than could possibly be incorporated in any set of standard resistivity curves. These standard curves provided the only means of interpretation by the curve matching techniques. The recent advances in electronics and the advent of high-speed computers made it possible to penetrate to large depths while using portable equipment, and to interpret the results without the limitations imposed by the standard resistivity curve albums. However, the interpretation of VES data, as well as all other resistivity data, is ambiguous. This fact will be stressed further in this report, but it is important to keep in mind that a unique interpretation can be made only when good control is available through wells which were drilled by means of modern drilling practices and logged by calibrated logging devices. Modern drilling practices ensure minimal changes in the properties of the strata penetrated by the well, and calibrated logging provides the true resistivities of the strata in absolute units.

The aim of this study is to determine the feasibility of using one of the VES methods—the Schlumberger array—on the coastal plain of southeastern Virginia for the following purposes: depth determination of the basement complex; location of freshwater horizons in the vicinity of the Dismal Swamp, the cities of Norfolk, Chesapeake, and Virginia Beach; and stratigraphic correlation. Thus, a total of 45 soundings were made throughout the area of Figure 1. Of these, three soundings (VES numbers 37, 41B, 42, and 43) were made close to wells (i.e., at or within five miles from the wells) with calibrated resistivity logs, two (VES numbers 40 and 44) close to wells with uncalibrated resistivity logs, one (VES 41A) close to a well with only a lithologic log, and two (VES numbers 1 and 2) at the seismic sites previously occupied by Costain and Robinson (1972).

THE COASTAL PLAIN REGION OF SOUTHEASTERN VIRGINIA

The coastal plain region of southeastern Virginia extends from the Fall Zone to the Atlantic coast (Figure 2). It is characterized by gently-eastward-sloping plains separated by north-northeast-trending scarps, of which the Surry and Suffolk scarps are the most conspicuous. These scarps extend northward to the Potomac River and southward into North Carolina.

Across the Fall Zone, elevations change from about 270 feet to about 120 feet within a few miles. Eastwards, abrupt changes in the elevation of 30 and 50 feet occur along the east-facing slopes of the Surry and Suffolk scarps.

The origin of the Surry and Suffolk scarps is not known with certainty. Oakes and Coch (1973, p. 25) suggest that the Suffolk scarp was formed by marine erosion of headlands; the Surry scarp, being a narrow ridge, probably formed as a barrier.

General Geology

The pre-Miocene geology of the coastal plain region of southeastern Virginia is not clearly understood. This is because outcrops are lacking, and the greatest majority of the wells in the area are shallow. Throughout the entire area of Figure 1, only the wells located close to the Fall Zone and the well at the town of Atlantic on the Eastern Shore (Figure 2) have penetrated the crystalline basement. The wells at Fort Monroe (drilled in 1902) and at the town of Mathews (drilled in 1929) are reported to have penetrated the crystalline basement at 2,246 and 2,325 feet, respectively, but recent gravity data (Sabet, 1972) suggest that these reports may not be correct.

In spite of the lack of data of unquestionable quality, it has long been assumed that the crystalline basement is a gently-eastward-sloping surface overlain by unconsolidated sediments of Cretaceous, Tertiary, and Quaternary ages, which appear to thicken gradually from a feather edge near the Fall Zone to 2,246 feet at Fort Monroe. This assumption was perpetuated in the literature as if it were reality.

Recently, gravity maps of southeastern Virginia were made and interpreted by the author (Sabet, 1972 and 1973). These interpretations suggest that the topography of the crystalline basement is rather complex. The interpretations were subsequently substantiated by the well at the town of Atlantic, which penetrated the basement at a depth of 6,174 feet, and by the well located to the south of Suffolk (near the North Carolina state line) (Figure 1), which was abandoned in sediments at a depth of 2,017 feet.

Figure 3 displays a generalized correlation diagram of the time-stratigraphic units encountered in the wells of the eastern portion of the study area. The extensive Cretaceous section found in the well at Atlantic, which is located in a gravity low (Sabet, 1973), and the presence of a thin Triassic section there, strongly suggest post-Triassic subsidence. Also, the thick Eocene section found in the Fort Monroe well in Hampton as compared to the thin section found in Moore's Bridge well in Norfolk led Cederstrom (1945) to suggest a pre-Eocene fault between Norfolk and Hampton. Later on, however, Cederstrom (1957, p. 25) stated that the thickness of the Eocene in the Fort Monroe well is not 800 feet, as reported earlier, but only about 125 feet, and that his previous reports were based on cuttings that were washed down from higher horizons during the drilling operation. Thus, since the crystalline basement was not reached in Norfolk at a depth of 2,585 feet (Brown, 1971), it is very unlikely that it was actually penetrated in the Fort Monroe well at a depth of 2,246 feet.

Occurrence of Groundwater

The groundwater resources of the area have been the subject of many state and federal publications. A partial list is included in the Bibliography, and a very brief summary is presented in Figure 4. The main source of this summary is the report published by the Virginia Division of Water Resources (Bull. 21, 1970).

According to the report, there are two main groundwater systems in the area—a shallow water-table system, and a deep artesian system. Both systems are separated from one another by essentially impermeable strata. The shallow system is being recharged by infiltration of surface water and precipitation. It is estimated that domestic wells withdraw about 15 million gallons per day from this system.

The sands and gravels of the Lower Cretaceous comprise the main artesian system in the area. These aquifers are recharged near the Fall Zone where they outcrop. It is estimated that industrial users withdraw 46 million gallons per day from the artesian system. However, this rate of withdrawal seems greater than the rate of replenishment. Thus, a large cone of depression, centered at Franklin, Virginia, has developed, where the artesian head has dropped from +20 feet in 1939 to -170 feet in 1969. It is estimated that, at the present rate of withdrawal, dewatering of these aquifers will begin by 1990.

The chloride content of the water of the artesian aquifers is less than 50 milligrams per liter (mg/l) at Franklin, increasing to 50 mg/l near Suffolk. Eastwards, it increases gradually from 50 to 500 mg/l within about 25 miles, and reaches 5,000 mg/l near the Atlantic coast, which is only 10 miles farther east.

These regional variations of the salinity do not reflect intense local variations which occur in the area extending eastwards from Suffolk. These local variations, when coupled with the lithologic variability which is characteristic of the Coastal Plain sediments, render the task of stratigraphic correlation based on VES interpretations east of Suffolk very tenuous. The salinity is relatively uniform west of Suffolk. Here the variability of the lithology is the major factor which limits correlations over large distances. However, correlations over short distances are possible.

THE SCHLUMBERGER ARRAY

The Schlumberger array has been used throughout this study. An outline of its theory is given below. This is followed by a discussion of the limitations of the resistivity sounding methods. The field methods are then presented together with a description of the instruments used. Finally, presentation of results and methods of interpretation are explained.

Theory

In the Schlumberger array (Figure 5), A and B are current electrodes, and M and N are potential electrodes. Let the current I enter the ground at A and return at B. Assuming the medium below the surface of the earth to be homogeneous and isotropic of resistivity ρ, the potentials V_M and V_N as measured at M and N, respectively, are given by:

$$V_M = \rho I/2\pi \;\; 1/(a - b/2) - 1/(a + b/2)$$

$$V_N = \rho I/2\pi \;\; 1/(a + b/2) - 1/(a - b/2)$$

from which $\rho = \pi(a^2/b - b/4)\ (V_M - V_N/I)$. Denoting $(V_M - V_N)$ by $\triangle V$, and acknowledging the fact that, in reality, the medium is anisotropic, the apparent resistivity ρ_a as measured by the Schlumberger array is given by:

$$\rho_a = \pi(a^2/b - b/4)\ \triangle V/I \qquad [1]$$

If a and b are measured in meters, and $\triangle V$ and I in millivolts and milliamperes respectively, ρ_a would be in ohm-meters (Ωm).

Equation (1) may be written as:

$$\rho_a = K/I\ \triangle V \qquad [1']$$

where $K = (a^2/b - b/4)$ is the geometric factor for the Schlumberger array. It can be shown (Keller and Frischknecht, 1966, p. 96) that by keeping the distance b less than 40% of a, the electric field E at the center of the spread is what is being measured by the Schlumberger array with an error of ±5%.

The electric field that will be measured by the Schlumberger array (AMNB) over an earth made of n homogeneous and isotropic layers of resistivities $[\rho_1, \rho_2 \ldots \rho_n]$ and thicknesses $[h_1, h_2 \ldots h_n]$ can' be calculated by the following formula:

$$E = -\rho_1 I/\pi \int_0^\infty F_{n-1}(m)\, J_1(ma)\, m\, dm$$

where ρ_1 = resistivity of uppermost layer,
I = current,
a = distance from center of spread to current electrode (Figure 5),
m = dummy variable,
$J_1(ma)$ = first order Bessel function,
$F_{n-1}(m)$ = a kernel function of depth to the lower boundary of each layer and the reflection coefficients.

The derivation of the above equation is rather complex. It is given by Keller and Frischknecht (1966, p. 144). Since $E \cong -\Delta V/b$, substitution in equation (1)′ yields:

$$\rho_a = \rho_1 Kb/\pi \int_0^\infty F_{n-1}(m)\, J_1(ma)\, m\, dm \qquad [2]$$

Several methods of evaluating equation (2), on a computer, have been devised. The computer program used in this work was given by Zohdy (1974).

Limitations

The interpretation of resistivity data is ambiguous. It is possible to find different combinations of thicknesses and resistivities which when substituted in equation [2] would yield the same theoretical resistivity sounding curve. (The ambiguity is exemplified by the alternative interpretations given for sites 5 and 37).

There are two main reasons for the ambiguity. The first is that in deriving equation [2] it was assumed that the earth is made of n homogeneous, isotropic, and horizontally continuous layers of resistivities $\rho_1, \rho_2, \ldots \rho_n$. If the layers are anisotropic (i.e., the resistivity of each layer in the vertical direction ρ_t differs from that in the direction parallel to bedding ρ_ℓ), it can be shown that the interpreted resistivity, from sounding data, of each layer is equal to neither ρ_t nor ρ_ℓ but equal to $\sqrt{\rho_t \rho_\ell}$ and its thickness is equal to the interpreted thickness divided by $\sqrt{\rho_t/\rho_\ell}$. Since ρ_t is generally greater than ρ_ℓ for horizontally layered media, the interpreted thickness would be greater than the true thickness.

Because an interpreter has no a priori knowledge of the exact number of layers which constitute the geoelectric section at a locality, it is customary to assume a number of layers ranging between three and six at the most. If the geoelectric section is made of many more layers than has been assumed, each of the interpreted layers would represent a grouping together of several layers. It can be shown that the layer which is equivalent to a group of homogeneous and isotropic layers is anisotropic. This layer is, in turn, equivalent to a homogeneous and isotropic layer whose thickness is greater than the thickness of an anisotropic layer by the factor $\sqrt{\rho_t/\rho_\ell}$ and whose resistivity is equal to $\sqrt{\rho_t\rho_\ell}$ (Kunetz, 1966).

To see these results, consider a model of a layered earth [Figure 6a] of a cross-sectional area of $1m^2$. Each layer is assumed to be homogeneous and isotropic. Their resistivities are given by $\rho_1\rho_2 \ldots \rho_n$, and their thicknesses are given by $h_1, h_2, \ldots h_n$. The tranverse resistance T† and the longitudinal conductance S† of this model are given by:

$$T = \sum_{i=1}^{n} \rho_i h_i$$

$$S = \sum_{i=1}^{n} h_i/\rho_i$$

Clearly, there is an infinite number of homogeneous and anistropic single layered models (Figure 6b) possessing the same values of S and T as the layered model (Figure 6a). Thus, depending on the chosen thickness h of the model, it is possible to find values for ρ_t and ρ_ℓ which satisfy the following relations:

---

† T and S as being used here should not be confused with the aquifer parameters T and S which correspond to transmissivity and storage, respectively. The storage coefficient is dimensionless and the transmissivity T=Kh where K and h are the hydraulic conductivity and aquifer thickness, respectively. However, a transformation of a layered aquifer can be made with respect to K in much the same was as it is done here with respect to ρ. Thus it can be shown (see for example, Harr, 1962) that a layered aquifer composed of n homogeneous and isotropic layers can be transformed into an equivalent single layered homogeneous anistropic aquifer such that:

$$K_\ell = \sum_{i=1}^{n} K_i h_i/h,$$

$$K_t = h/\sum_{i=1}^{n} h_i/K_i$$

where K_ℓ and K_t are the longitudinal and transverse hydraulic conductivities, respectively. Also, by distorting the aquifer's thickness by the factor $\sqrt{K_\ell/K_t}$, or its width by the factor $\sqrt{K_t/K_\ell}$, one obtains an equivalent single layered aquifer which is homogeneous and isotropic, of conductivity $K = \sqrt{K_\ell K_t}$.

$$T = \rho_t h \quad [5]$$

and $$S = h/\rho_\ell \quad [6]$$

Let $h^* = \sum_{i=1}^{n} h_i$ and let ρ_t^* and ρ_ℓ^* be the corresponding values of ρ_t and ρ_ℓ as determined by the relations [5] and [6], respectively. It is clear then that the model of Figure 6b is equivalent to that of Figure 6a in S and T. Both models are of the same thickness, but one model is composed of several homogeneous and isotropic layers, and the other is made of a single homogeneous and anisotropic layer.

To find a homogeneous and isotropic model which is equivalent in S and T to the original model, and consequently equivalent to the second model, we proceed as follows. Let ρ and H be the resistivity and thickness of the required model; then

$$T = \rho_t^* h^* = \rho H \quad [7]$$

and $$S = h^*/\rho_\ell^* = H/\rho \quad [8]$$

From the relations [7] and [8], the following results can be obtained:

$$H = h^* \sqrt{\rho_t^*/\rho_\ell^*} \quad [9]$$

$$\rho = \sqrt{\rho_t^* \rho_\ell^*} \quad [10]$$

Relations [8] and [9] show that if a medium is assumed to be homogeneous and isotropic, while in reality it is homogeneous and anisotropic, its calculated thickness would be greater than its true thickness by the factor $\sqrt{P_t/P_\ell}$, and its calculated resistivity would be equal to $\sqrt{\rho_t \rho_\ell}$.

The second major source of ambiguity stems from the assumption of lateral continuity, and from the fact that since the distance MN is finite, the accuracy of measuring the electric field E is about ±5%. Lateral inhomogeneities are reflected, on the apparent resistivity curve, by cusps and by jumps accompanying changes in the distance MN. The observed VES curve can thus be interpreted in different ways such that the resulting theoretical curve does not differ from the observed one by more than ±5%. This is known as the principle of equivalence. It has been clearly explained by Bhattacharya and Patra (1968, p. 61), and by Keller and Frischknecht (1966, p. 158), who show, for example, that the apparent resistivity curves for the sections shown in Figure 7 are equivalent.

The principle of suppression (Figure 8) is another important principle which must be clearly understood for proper evaluation of the interpretations of resistivity sounding curves. According to this principle (Kunetz, 1966, p. 58), a thin bed whose resistivity is intermediate between the overlying and underlying resistivities has no effect on the resistivity curve. Thus, a thin freshwater-saturated sandstone overlain by a thick section of shale and underlain by the basement complex may have no effect on the shape of the resistivity sounding curve and therefore may not be detected by the resistivity method. Furthermore, an increase in thickness of the freshwater sand would be indistinguishable from a change in thickness or resistivity of the shale.

Flathe (1963) showed still another important limitation of resistivity soundings in regard to the detection of successive groundwater aquifers. The sequence which he investigated was made of the following layers (top to bottom): a surface layer of gravel, an upper sandstone aquifer, a thin clay unit, a lower sandstone aquifer, and a very thick shale unit. He concluded that if the thickness of the uppermost aquifer exceeds that of the lower one, the latter cannot be detected. If both aquifers are of the same thickness, the lower one is detectable only if the near surface layer is resistant and the conductance of the clay unit separating the two aquifers is very high.

In spite of these drawbacks, the resistivity method does provide a unique measure of one property of the subsurface strata; namely, that of the longitudinal conductance S (defined by equation 4). Keller and Frischknecht (1966, p. 114) show that in case of a sequence of conductive sedimentary rocks of thickness h and resistivity ρ, underlain by a resistant crystalline basement complex, the apparent resistivity ρ_a as measured by the Schlumberger array at large electrode separations a of about twice the thickness h, is given by:

$$\rho_a = (\rho/h)a \qquad [11]$$

By taking the logarithm of both sides of (11), we get:

$$\log \rho_a = \log \rho/h + \log a \quad \text{or}$$
$$\log \rho_a + \log h/\rho = \log a \qquad [12]$$

Thus, by plotting ρ_a versus a on log-log graph paper, a straight line sloping at an angle of 45° would be obtained. The value of a obtained at the intersection of this line and the line $\rho_a = 1$ is equal to S.

It is not necessary to actually obtain the 45° sloping line in order to determine S. The minimum value of S can be obtained by drawing a 45° line from the apparent resistivity value which corresponds to the largest spacing "a" attained in the field.

Although in deriving equation (11) the resistivity of the basement was assumed to be infinite, in practice a resistivity of a thick layer 20 to 30 times the resistivity of the overlying layer is sufficient to cause a 45° rise in the apparent resistivity curve to occur. Thus, an "electric basement" may be reached within the sedimentary sequence, and no information about the underlying sedimentary sequence can be obtained by galvanic resistivity methods.

In a multi-layer sequence, a thin conductive layer overlying the "electric basement" will not be detected. Thus, the resistivity of the "electric basement" will be erroneously interpreted as 20 to 30 times the overlying thick layer which has been detected while, in fact, its resistivity is only about 10 times, or less, that of the layer (Figure 9).

Finally, the reader is cautioned against making any a priori quantitative inferences based on the shape of the resistivity sounding curve. Figure 10 depicts two completely different curves for two resistivity models which are essentially the same. The only difference is that in one case a thin, less resistant layer has replaced the upper part of the near surface layer of the other model, as might be expected to occur due to changes in facies.

Field Methods

The sites were chosen along county and farm roads where 8,000-foot-long straight stretches are found and believed to be free from buried cables and pipes. Where the depth to the basement complex was estimated to be within 1,500 feet, a straight stretch of 6,000 feet was found sufficient. The center point of the spread was located approximately at the middle of the chosen straight stretch of road. From this point the following distances (in feet) were measured in each direction along the road: 10, 14, 20, 25, 30, 40, 50, 65, 80, 100, 140, 200, 250, 300, 400, 500, 650, 800, 1,000, 1,400, 2,000, 2,500, 3,000, and 4,000. These distances were chosen such that the difference between the logarithms of any two consecutive distances is nearly a constant. For example, the difference between log 100 and log 80 is approximately equal to the difference between log 50 and log 40. Accordingly, these distances should have been chosen at 10, 12, 16, 20 . . . etc., but in this work a distance of 14 was substituted for both 12 and 16.

A 2-foot electrode, made of stainless steel, was driven into the soil at each end of the spread (A & B, Figure 5). Both electrodes were then connected to the current sender, located at the center, by two 16-gauge cables. The electrodes M and N (Figure 5) were also driven into the soil and connected to the voltage receiver, at the center, by two coaxial cables whose shieldings were grounded at the center. The distance MN was kept equal to or less than 0.2 AB.

The current sender used in this work was manufactured by Geoexploration of Tucson, Arizona. The current source was a 2-kilowatts, 400-volts, 400-cycles generator manufactured by ALLECO Corporation of New York. The generator was driven by a 4-horsepower gasoline engine. The sender is designed to send current accurately between 100 milliamperes and 4 amperes in steps as low as 0.1 milliamperes. The current output of the sender is in the form of a square wave. A selector allows for selecting any of the following frequencies: D.C., 0.05 Hz, 0.1 Hz, and 3 Hz. The 0.5 and 0.1 cycles were used in this work.

Two voltage receivers were used. The first, also manufactured by Geoexploration, can receive accurately between 1.5 millivolts and 15 volts. It is tuned for the 0.5 Hz frequency and equipped with a D.C. bucking circuit which is made for bucking self-potential (SP) voltages arising from natural currents. The second receiver is a potentiometer recorder manufactured by Honeywell. It records voltages accurately between 100 microvolts and 100 volts. This receiver lacks the SP bucking circuit, but with the proper connections made between the Honeywell and the Geoexploration receivers, the SP bucker of the latter was used by the former; its filters and amplifiers were also utilized by the Honeywell device to further enhance the signal and to extend its range to 10 microvolts. The Honeywell device, however, operates on 100 volts, 60 Hz current. Thus a sinusoidal power converter manufactured by Cornell-Dubilier was used, together with a Sears Die-Hard 12-volt battery.

The fieldwork required three men. Two men taped the distances, laid the cable, and moved and stood by the two current electrodes A & B. The third man, the observer, remained at the center point; he was responsible for taking the measurements and for moving the electrodes M and N. Contact between the three men was established by 5-watt transreceivers. Since the currents and voltage sent into the ground through A and B could be fatal, it was necessary to keep a man near each electrode lest someone should accidentally step over the electrode. There was no danger of accidentally severing the current cable, because the current sender is equipped with a safety device that will turn off the circuit whenever the resistance increases above a certain value.

At each position of A and B, the observer recorded the frequency used, the current sent, the voltage received, and the distances AB and MN. Except for the frequency, these are the data needed to calculate the apparent resistivity

ρ_a by equation (1). Occasionally the frequency 0.1 Hz was used in addition to the 0.5 Hz. This was done to check on the system and to check for any dependence of the measured resistivity on frequency, a situation which can arise if the rocks contained disseminated mineral sulfides.

Presentation of Results

From the field data, the apparent resistivity ρ_a was calculated using equation (1) and plotted versus AB/2 on log-log paper. Among the advantages of the log-log plot is that it emphasizes near-surface resistivity variations and suppresses variations at greater depths. This is important, because interpretation of the results depends largely on the small variations in resistivity occurring at shallow depths. Another advantage of the log-log plot is that if at two different sites the resistivities of the underlying layers (or their thicknesses) increase or diminish by the same constant multiple, the two resistivity curves would look alike, although they may be shifted horizontally or vertically with respect to one another. In addition, the basement complex or the presence of an electric basement is readily determined on the log-log plot by a 45° sloping straight line as predicted by equation (12).

Interpretation Methods

The interpretation of each VES curve was carried out in two steps. First, an approximate interpretation was obtained by the curve-matching methods described by Orellana and Mooney (1966), and another interpretation was obtained through the use of an automatic interpretation computer program (Zohdy, 1972). Based on these interpretations, the parameters ρ and h of a geoelectric model, thought to be closer to reality, were estimated, substituted in a computer program of equation (2), and modified by trial and error until a very close match was attained between the calculated and observed resistivity curves. The best model is given in the Appendix, together with the measured VES curve at each site.

The automatic curve-matching computer program results in a geoelectric model the calculated apparent resistivity of which matches the given field curve almost exactly. Thus, the interpretation as determined by the program is mathematically correct but may not necessarily correspond to reality. The number of layers as determined by the program is about ten. The resistivities of some of these layers are sometimes unrealistically small or large, while their thicknesses are too small to be detected by the VES methods. In other words, the results may, on some occasions, tend to exceed the limitations of the VES methods. Nonetheless, the geoelectric model determined by the program helps in estimating the parameters of a four- or five-layer model whose apparent resistivity matches the field data. The outputs from this program are correlated with the corresponding resistivity logs of the sites numbers: 37, 40, 42, and 43 (Figure 11) and are given in the Appendix for sites 5, 37, and 40-44.

Zohdy (l969, p. 723) presented a method of interpretation which he obtained from the Russian literature. It is applicable to H-type geoelectric sections ($\rho_1 > \rho_2 > \rho_3$) in which the thickness of the middle layer h_2 is at least three times the thickness of the first layer ($h_2 > 3h_1$). The method consists of determining the longitudinal conductance S from the VES curve as explained earlier and then transforming the VES curve as obtained by the Schlumberger array into the corresponding curve which would have been obtained by the dipole polar sounding array (DPS). The apparent resistivity at the minimum $\rho_{mín}$ on the DPS curve is equal to ρ_ℓ, the longitudinal resistivity. Since S = H/ρ_ℓ, the depth H to the basement complex can then be calculated.

The transformation of the VES curve into a DPS curve is accomplished by first dividing the abscissa of the VES curve at a logarithmic interval of $\sqrt{2}$ (i.e., the log of any abscissa minus the log of the abscissa preceeding it must equal log $\sqrt{2}$), and then calculating the apparent DPS resistivity value (ρ_{DPS} at each point by the formula:

$$\rho_{DPS} = \rho_o \,(1 - 2.2146 \log\, (\rho_{-1} \,/\, \rho_{+1}) + 0.2768 \log \rho_{+2}/\rho_{-2})$$

where ρ_o	=	the apparent resistivity on the VES curve at the point whose apparent DPS resistivity value is being sought;
ρ_{-1}, ρ_{+1}	=	the apparent resistivities on the VES curve which correspond to the abscissa on the left and right of ρ_o,respectively; and
ρ_{-2}, ρ_{+2}	=	the apparent resistivities on the VES curve which correspond to the abscissa on the left and right of ρ_{-1} and ρ_{+1}, respectively.

This method has been applied to the resistivity curve of site number 1 (Figure 12). The depth to the basement of 1,200 feet as determined by this method is closer to the seismic depth of 950 feet (Costain and Robinson, 1972) than the depth obtained through direct interpretation of the VES curve (see Appendix).

RESULTS AND DISCUSSION

From this study, several conclusions can be made. Perhaps the most important conclusion is that vertical electrical resistivity soundings (VES) do provide adequate and inexpensive means of studying the subsurface in the coastal plain region of southeastern Virginia; and, notwithstanding inherent inaccuracies caused by lateral inhomogeneities and anisotropism, interpretation of VES data leads to the knowledge of the maximum depth below which it would be unlikely for groundwater aquifers to occur. This is because the resistivity of water-bearing sands depends mainly on the salinity of the water, the degree of saturation, and the presence of clays and silts. The resistivity of clean sands (not containing shale or silt) and gravel saturated with fresh water ranges between 20 and several hundred ohm-meter. On the other hand, the resistivity of the same sand containing silt, clay, or brackish water is much lower. It is thus established that fresh groundwater is unlikely to be produced from horizons of resistivity less than 10 ohm-meter. From the resistivity logs of the wells at Moore's Bridge (Norfolk) and Lee Hall, Brown (1971) concluded that the resistivity of freshwater-bearing horizons (water containing less than 1,000 mg/l of dissolved solids) varies between 19 and 25 ohm-meter. However, the resistivity of a layer as determined from a VES curve may not necessarily be the same as the one measured by the well-logging device. This is because the well-log resistivity includes all the extraneous effects introduced by the drilling operation. A better estimation of the lower limit of the resistivity at which fresh water may occur would be through statistical correlation between VES resistivities and the known occurrences of freshwater-bearing horizons in wells. Unfortunately, the available well data in the coastal plain of southeastern Virginia do not permit such correlation.

The only sounding in the area that can be correlated to reliable well data is that of VES 37, located about one-half mile from the 2,017-foot-deep well near Suffolk (Figure 1). The quality of this sounding curve is indeed very low, even though it is the best of the two soundings made in that area (the other one is VES 4). Nonetheless, the alternative interpretation, provided by Zohdy's automatic interpretation program (Figure 11 and Appendix) shows a layer of resistivity of 16 ohm-meter between the depths 416 and 1,171 feet. The lowermost occurrence of fresh water in this well is between 696 and 790 feet. Brackish waters with a chloride content of 11,000 and 14,000 mg/l occur in the intervals 947 to 952 and 1,115 to 1,120 feet, respectively. In other words, the resistivity of 16 ohm-meter extends throughout a horizon which includes both fresh and brackish waters. This is an example for the principle of suppression. Thus, it seems that, in order to be on the safe side, a choice of 20 ohm-meter as the cutoff limit for the occurrence of fresh water should be adopted with the knowledge that this choice was made on the basis of one well only, and that freshwater horizons could be associated with resistivities lower than 20 ohm-meter. Therefore, the interpretations which follow should be considered *tentative*.

In the vicinity of the Dismal Swamp, potential aquifers are expected only within a thin veneer of sediments ranging in thickness between 20 and 40 feet. This conclusion is based on the interpretation of the VES curves numbers 20, 22, 35, 36, and 38. These results strongly suggest that the Dismal Swamp is *not* an area of aquifer recharge.

To the east of the Dismal Swamp, the maximum depth of fresh groundwater aquifers appears to increase to 130 feet and then diminish toward the Atlantic coast to 43 feet (site 39). However, the increase in depth is not uniform. For example, at sites 5 and 6 the interpretations suggest maximum depths of 20 and 30 feet, respectively, whereas at sites 3 and 7 the depths appear to be 50 and 80 feet, respectively. The maximum thickness is attained at sites 20, 25, and 29. An alternative interpretation is presented for the data of site 5 in order to stress the idea that the interpretations being discussed are not unique.

To the north and northeast of the Dismal Swamp, the maximum depth to potential groundwater aquifers appears to diminish from 85 feet (sites 3 and 19) to 60 feet (site 24.)

Northward from the Dismal Swamp, interpretation of the VES curves at sites 32 and 34 suggests that the maximum depth to potential aquifers increases to 180 feet (site 32), then diminishes to 110 feet (site 34).

To the west of the Dismal Swamp, interpretation of the VES curve number 26 suggests that the maximum depth to potential aquifers is about 55 feet. Westward, the maximum depth increases to 315 feet at site 13.

In the vicinity of the town of Gloucester, the thickness of the sedimentary section which may contain groundwater aquifers is, generally, large. To the south and north of Gloucester it is found to be 500 feet (site 8) and 600 feet (site 11), respectively. To the east of Gloucester, the thickness appears to reach a maximum of 1,730 feet (site 9), then diminishes to 140 feet to the east of the town of Mathews (site 10).

In the vicinity of the town of Painter on the Eastern Shore the maximum depth to groundwater aquifers appears to range between 920 feet (site 15) and 560 feet (site 16).

The occurrence of groundwater aquifers at depths greater than those stated in the previous paragraphs should not be ruled out. It is reasonably certain that the crystalline basement has been detected at sites 1, 2, 9, 12, 13, 14, 40, 41-A, 41-B, and 43. At all the other sites the rise of the apparent resistivity curve associated with larger values of AB/2 is interpreted to reflect an "electric basement" which could represent a resistant bed embedded in a conductive horizon, a freshwater horizon, or the crystalline basement proper.

An example of this electric basement is given by VES 42, located five miles from the well at Atlantic. Because the crystalline basement in this well was reached at a depth of 6,172 feet, the basement at 1,610 feet (as given by the interpretation of VES 42) must be an electric basement. The well log (Figure 11) does not show a thick layer whose resistivity is 80 ohm-meter (or larger) at 1,600 feet. It shows an abrupt increase in resistivity at about 1,400 feet from less than 2 to 6 ohm-meter, which seems to persist to greater depths. A threefold increase in resistivity is insufficient to cause the right-hand portion of the VES curve to rise at an angle of 45°. It may, however, cause a rise of as much as 25°. Therefore, either the resistivity below 1,400 feet in the well is much higher than that recorded in the well log, or that the VES data obtained at distances AB/2 greater than 2,500 feet contained noise which caused the sounding curve to rise at an angle of 45° rather than 25°. If the interpreted depths correspond to reality, the difference in depth between 1,400 feet at the well and 1,600 feet at the VES site can be explained in terms of a dip angle which is less than ½°.

The depths of the basement at sites 1 and 2 are shown to be 1,450 and 850 feet, respectively. On the basis of the seismic study made at these sites (Costain and Robinson, 1972), the respective depths of 990 and 575 feet are determined. Since the interpretation of seismic data depends on the estimated velocity function, it can be concluded only that if the seismic depths are correct, then the coefficient of electric anisotropy at the two sites is about 1.50. This value is very high. In fact, a coefficient of 1.1 of 1.2 is more likely for the Coastal Plain sediments (Zohdy, personal communication). Examination of Figure 11 shows that at the VES sites numbered 40 and 43, the VES basement depths are close to those actually found by drilling.

Examination of the logs shown in Figure 11, together with the VES interpretations, leads to the interesting conclusion that there seem to be good correlations between the variations in the VES resistivities and the well-log resistivities. However, because of the variability of the sediments and water salinity in the area, it is unlikely that detailed stratigraphic correlations over large distances can be made on the basis of VES interpretation.

BIBLIOGRAPHY

Bhattacharya, P.K., and Patra, H.P., 1968. Direct Current Geoelectric Sounding, Principles and Interpretation. Elsevier Pub. Co., New York, 135 pp.

Brown, D.L., 1971. Techniques for Quality-of-Water Interpretations from Calibrated Geophysical Logs, Atlantic Coastal Area. Ground Water 9(4):28-38.

Brown, P.M., et al., 1972. Structural and stratigraphic framework, and spatial distribution of permeability of the Atlantic Coastal Plain, North Carolina to New York. USGS Prof. Paper 796, 79 pp.

Cederstrom, D.J., 1945. Structural geology of southeastern Virginia. Am. Assoc. Petroleum Geologists Bull. 29(1):71-95.

Cederstrom, D.J., 195. Geology and ground-water resources of the York-James Peninsula, Virginia. U.S. Geological Survey Water Supply Paper 1361, 237 pp.

Costain, J.K., and Robinson, E.S., 1972. Some Seismic Measurements on the Virginia Coastal Plain. Water Resources Research Center Bulletin 56, Blacksburg, Virginia. 69 pp.

Cushing, E.M., et al., 1973. Water Resources of the Delmarva Peninsula. USGS Prof. Paper 822, 58 pp.

DeBuchananne, G.D., 1968. Ground-water resources of the Eastern Shore of Virginia and the James, York, and Rappahannock river basins of Virginia east of the fall line. U.S. Geological Survey Hydrol. Inv. Atlas HA-284.

Harr, M.E., 1962. Groundwater and Seepage. McGraw-Hill Books, New York, New York.

Keller, G.V., and Frischknecht, F.C., 1966. Electrical Methods in Geophysical Prospecting. Pergamon Press, 517 pp.

Krumbein, W.C., and Sloss, L.L., 1963. Stratigraphy and Sedimentation. W. H. Freeman and Co., San Francisco, 660 pp.

Kunetz, G., 1966. Principles of Direct Current Resistivity Prospecting. Gebruder Borntraeger, Berlin-Nikolassee, 103 pp.

LeGrand, H.E., 1961. Summary of geology of Atlantic Coastal Plain. Am. Assoc. Petroleum Geologists Bull. 45(9):1557-1571.

Oakes, R.Q., Jr., and Coch, N.K., 1973. Post-Miocene stratigraphy and morphology, Southeastern Virginia. Virginia Division of Mineral Resources Bull. 82, 135 pp.

Orellana, E., and Money, H.M., 1966. Master Tables and Curves for Vertical Electrical Sounding Over Layered Structures. Interciencia, Costanilla de Los Angeles, 15, Madrid, Spain.

Sabet, M.A., 1972. Basement configuration in Southeastern Virginia. Presented at the 85th Annual Meeting of the Geological Society of America, Minneapolis, Minnesota, Abs. With Programs 4(7):649.

Sabet, M.A., 1973. Gravity and magnetic investigation, Eastern Shore Area, Virginia. Geol. Soc. America Bull. 84:2119-2126.

Virginia Department of Conservation and Economic Development, 1970. Groundwater of Southeastern Virginia. Division of Water Resources Bull. 261, p. 54.

Zohdy, A.A.R., 1969. The use of Schlumberger and equatorial soundings in groundwater investigations near El Paso, Texas. Geophysics 34(5):713-728.

Zohdy, A.A.R., 1973. A computer program for automatic interpretation of Schlumberger sounding curves over horizontally stratified media. PB-232703, National Technical Information Service, Springfield, Virginia. 25 pp.

Zohdy, A.A.R., 1974. A computer program for the calculation of Schlumberger sounding curves by convolution. PB-232056, National Technical Information Service, Springfield, Virginia. 11 pp.

SUMMARY OF PERTINENT DATA AND INTERPRETATIONS

Locations of Resistivity Soundings
Coastal Plain Region, Southeastern Virginia

Site No.	Latitude	Longitude	Quandrangle	Remarks
1	36°45.02′	76°52.87	Sedley	County Rd. 630
2	36 37.23	77 11.28	Boykins	Hwy 35 at Cross Keys
3	36 30.45	76 21.38	Lake Drummond SE	Hwy 17
4	36 34.91	76 35.14	Corapeake	Hwy 32
5	36 42.50	76 20.07	Deep Creek	Hwy 104
6	36 36.67	76 19.55	Lake Drummond SE	Lake Drummond Cswy.
7	36 39.00	76 21.53	Deep Creek	West Landing Rd.
8	37 22.98	76 31.41	Gloucester	County Rd. 615
9	37 25.28	76 28.40	Ware Neck	Farm Rd. off 623
10	37 26.07	76 17.26	Mathews	County Rd. 644
11	37 30.60	76 40.75	Shacklefords	Hwy 14
12	36 44.98	77 15.77	Drewryville	County Rd. 308
13	36 50.04	77 17.40	Yale	County Rd. 735
14	37 05.70	77 26.19	Reams	County Rd. 606
15	37 36.63	75 17.76	Exmore	Hwy. 180
16	37 34.28	75 43.15	Wachapreague	N. of Quinby
17	37 26.68	76 54.19	Walkers	County Rd. 603
18	37 06.25	76 25.49	Newport News	Hwy 134
19	36 47.13	76 06.32	Princess Anne	Princess Anne Rd.
20	36 38.70	76 06.78	Pleasant Ridge	Land of Promise Rd.

21	36 22.17	76 26.29	Elizabeth City, N.C.	Paved Rd. Dismal Swamp
22	36 19.35	76 04.81	Elizabeth City, N.C.	Paved Rd.
23	36 16.31	76 25.39	South Mills, N.C.	Dirt Rd.
24	36 43.68	76 04.57	Pleasant Ridge	Indian River Rd.
25	36 37.98	76 11.03	Fentress	Head of the River Rd.
26	36 36.97	76 34.35	Corapeake	County Dirt Rd.
27	36 37.31	76 08.78	Moyock	Head of the River Rd.
28	36 34.27	76 06.90	Creeds	Paved Rd.
29	36 30.16	76 12.58	Moyock	Farm Rd., N.C.
30	36 38.81	76 16.23	Deep Creek	Paved Rd.
31	36 41.22	76 17.87	Deep Creek	Paved Rd.
32	36 50.45	76 34.70	Chuckatuck	County Road 603
33	36 46.67	76 25.88	Bowers Hill	Rd. S of Norfolk & Western RR
34	36 55.44	76 32.54	Benn's Church	County Rd. 664
35	36 42.18	76 31.62	Suffolk	Lynn Rd., Dismal Swamp
36	36 37.86	76 29.53	Lake Drummond NW	Washington Ditch, Dismal Swamp
37	36 34.63	76 35.09	Corapeake	Hwy 32
38	36 36.72	76 31.58	Corapeake	West Rd., Dismal Swamp
39	36 32.14	76 51.74	Knotts Island	West of sand dunes
40	36 34.87	76 50.28	Gates	County Rd. 667
41A	36 57.05	77 01.43	Manry	County Rd. 620
41B	36 58.86	77 08.97	Littleton	Hwy 40
42	37 57.43	75 36.90	Hallwood	County Rd. 701
43	37 21.25	77 06.35	Charles City	County Rd. 618
44	37 34.63	76 46.40	West Point	County Rd. 657

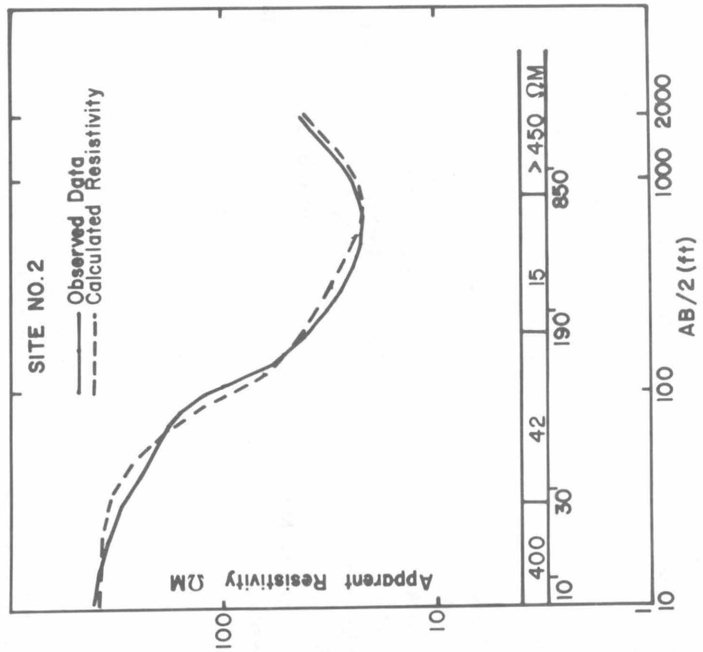
SITE NO.2
Observed Data
Calculated Resistivity
Apparent Resistivity ΩM
100
10
400
42
15
> 450 ΩM
10
30
190
850
10
100
1000
2000
AB/2 (ft)

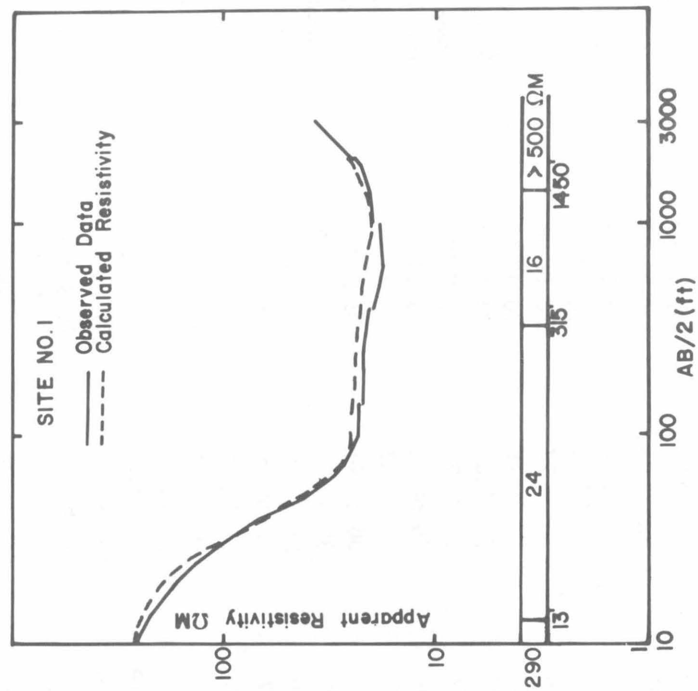
SITE NO.1
Observed Data
Calculated Resistivity
Apparent Resistivity ΩM
100
10
290
24
16
> 500 ΩM
13
315
1450
10
100
1000
3000
AB/2 (ft)

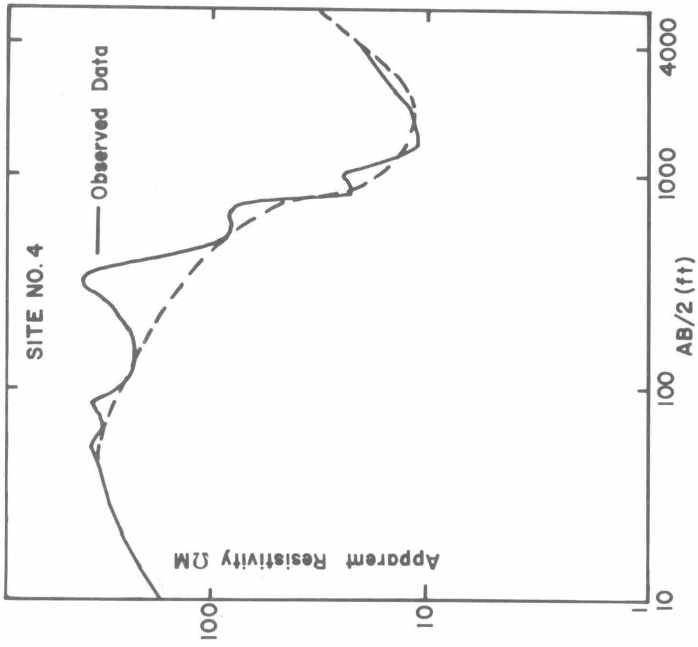
SITE NO. 4
Observed Data
Apparent Resistivity ΩM
100
10
1
10
100
1000
4000
AB/2 (ft)

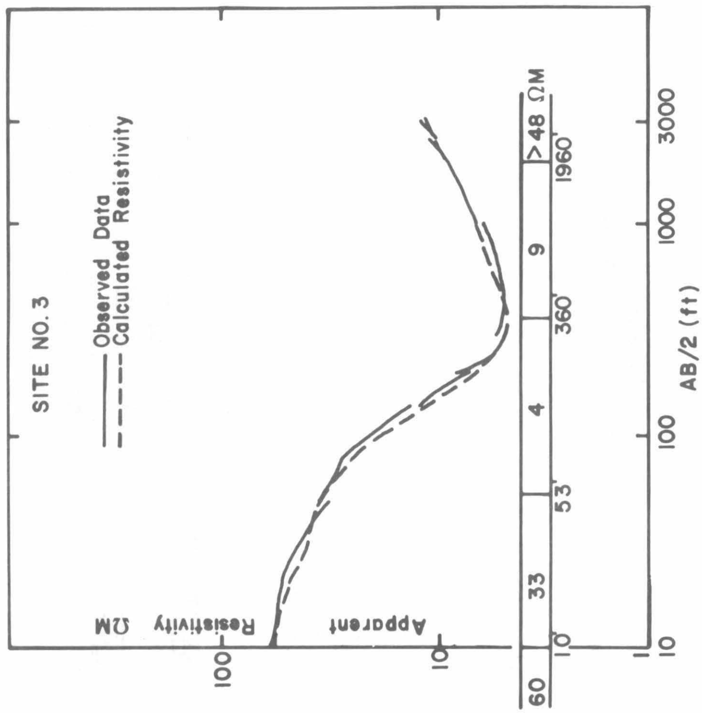
SITE NO. 3
Observed Data
Calculated Resistivity
Apparent Resistivity ΩM
100
10
1
10
100
1000
3000
AB/2 (ft)
60
10
33
53
4
360
9
1960
>48 ΩM

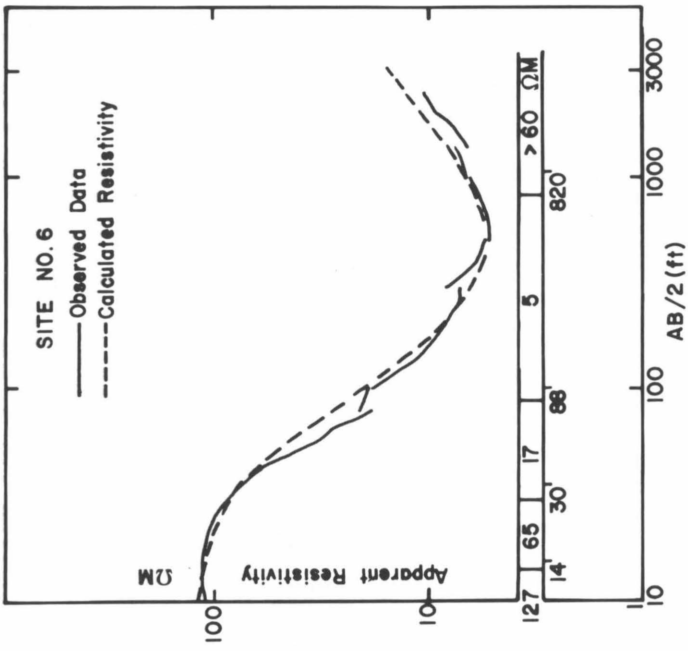
SITE NO. 6
Observed Data
Calculated Resistivity
ΩM
Apparent Resistivity
100
10
10
100
1000
3000
AB/2 (ft)
127
14
65
30
17
88
5
820
>60 ΩM

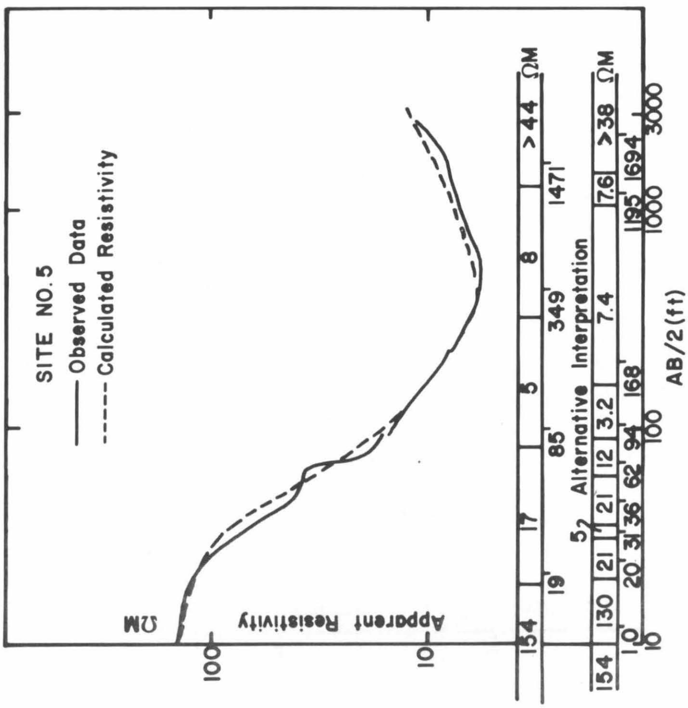
SITE NO. 5
Observed Data
Calculated Resistivity
ΩM
Apparent Resistivity
100
10
10
100
1000
3000
AB/2 (ft)
154
19
17
85
5
349
8
1471
>44 ΩM
Alternative Interpretation
154
130
21
21
12
3.2
7.4
7.6
>38 ΩM
10
20
31
36
62
94
168
1195
1694

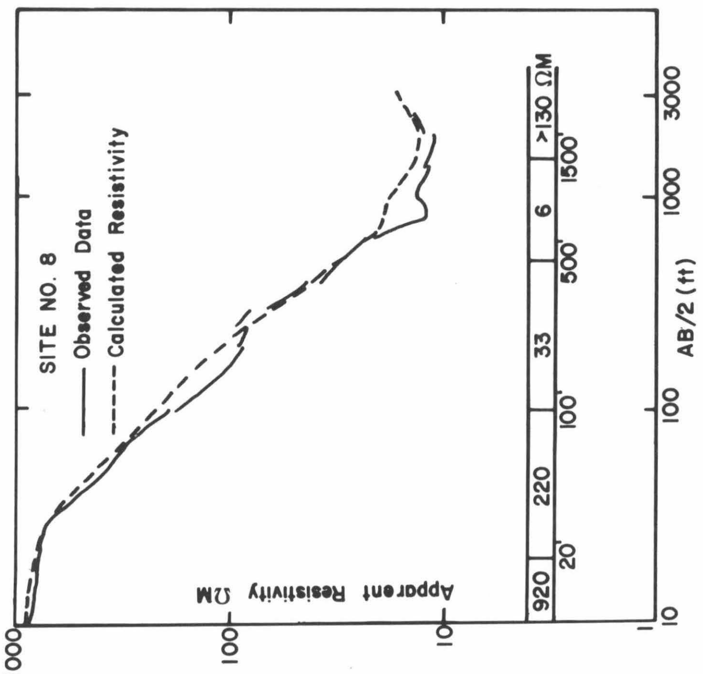
SITE NO. 8
Observed Data
Calculated Resistivity
Apparent Resistivity ΩM
1000
100
10
1
10
100
1000
3000
AB/2 (ft)
920
20
220
100
33
500
6
1500
>130 ΩM

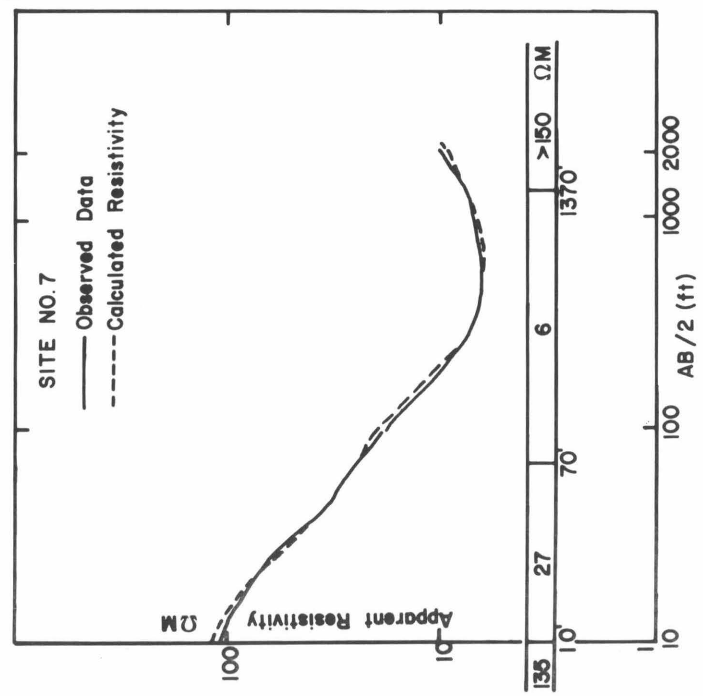
SITE NO.7
Observed Data
Calculated Resistivity
Apparent Resistivity ΩM
100
10
1
10
100
1000
2000
AB/2 (ft)
135
10
27
70
6
1370
>150 ΩM

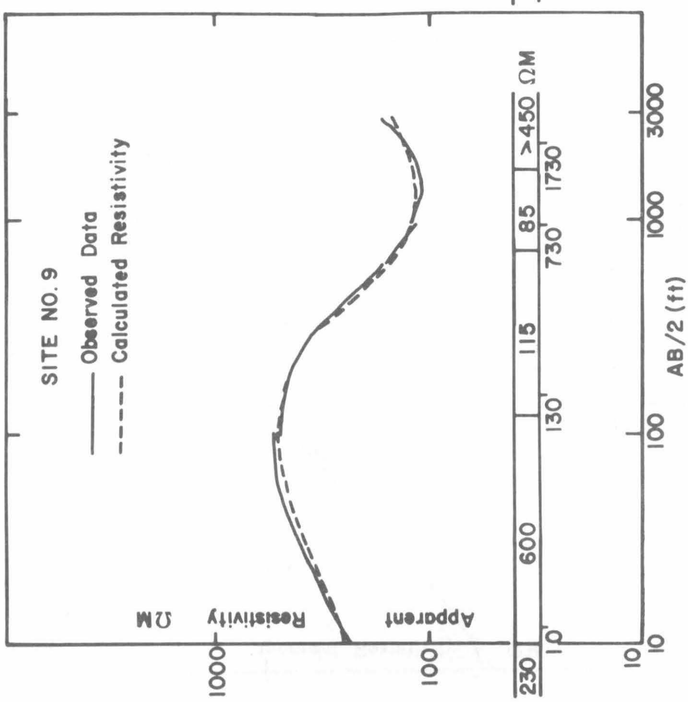
SITE NO. 9
Observed Data
Calculated Resistivity
Apparent Resistivity ΩM
1000
100
10
100
1000
3000
AB/2 (ft)
230
10
600
130
115
730
85
1730
>450 ΩM

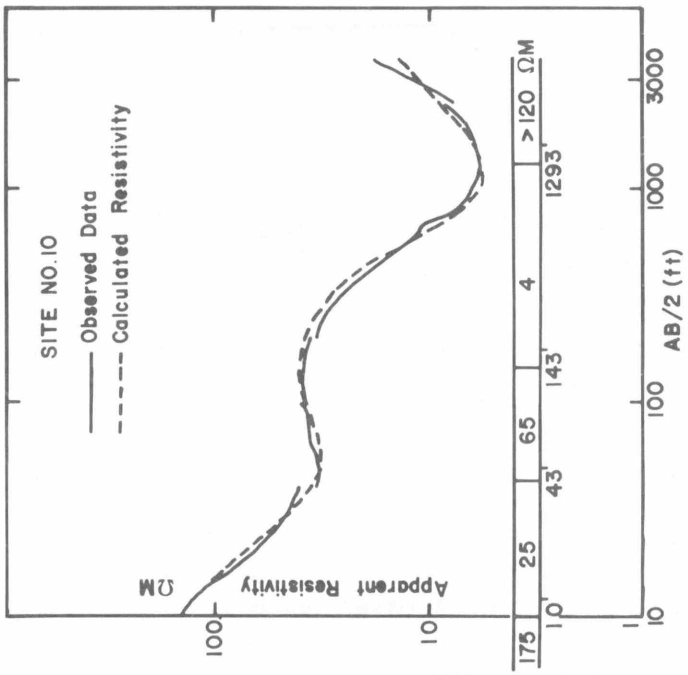
SITE NO. 10
Observed Data
Calculated Resistivity
Apparent Resistivity ΩM
100
10
1
10
100
1000
3000
AB/2 (ft)
175
10
25
43
65
143
4
1293
>120 ΩM

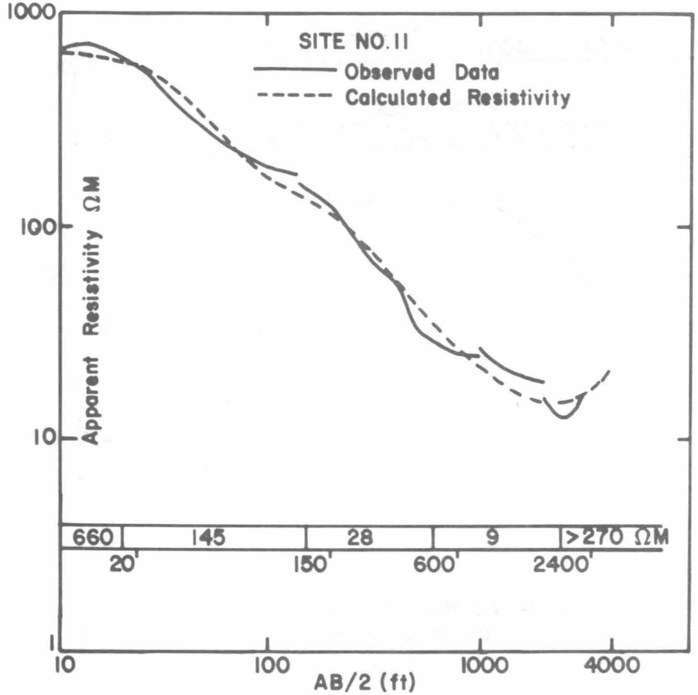
SITE NO.11
Observed Data
Calculated Resistivity
Apparent Resistivity ΩM
1000
100
10
1
660
145
28
9
>270 ΩM
20
150
600
2400
10
100
1000
4000
AB/2 (ft)

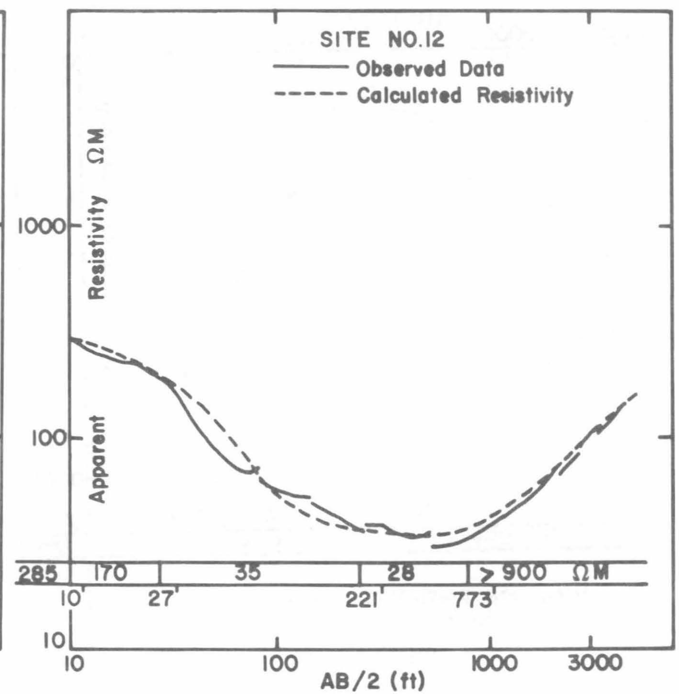
SITE NO.12
Observed Data
Calculated Resistivity
Apparent Resistivity ΩM
1000
100
10
285
170
35
28
> 900 ΩM
10
27
221
773
10
100
1000
3000
AB/2 (ft)

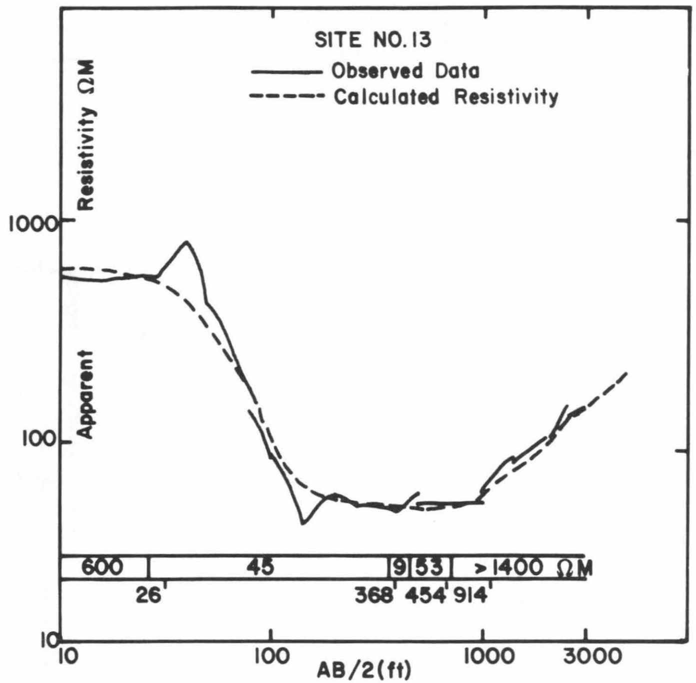
SITE NO. 13
Observed Data
Calculated Resistivity
Apparent Resistivity ΩM
1000
100
10
600
45
9
53
>1400 ΩM
26
368
454
914
10
100
1000
3000
AB/2(ft)

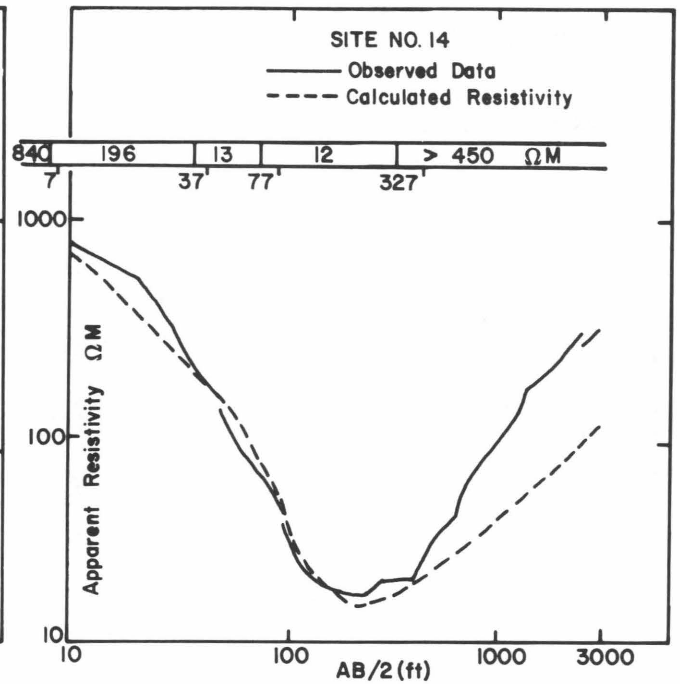
SITE NO. 14
Observed Data
Calculated Resistivity
840
196
13
12
> 450 ΩM
7
37
77
327
1000
100
10
Apparent Resistivity ΩM
10
100
1000
3000
AB/2 (ft)

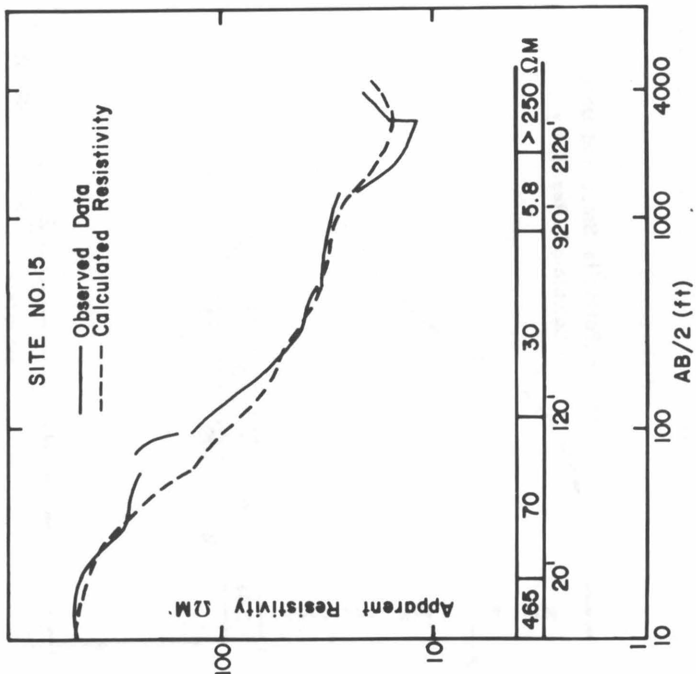
SITE NO. 15
Observed Data
Calculated Resistivity
Apparent Resistivity ΩM.
100
10
1
10
100
1000
4000
AB/2 (ft)
465
70
30
5.8
>250 ΩM
20
120
920
2120

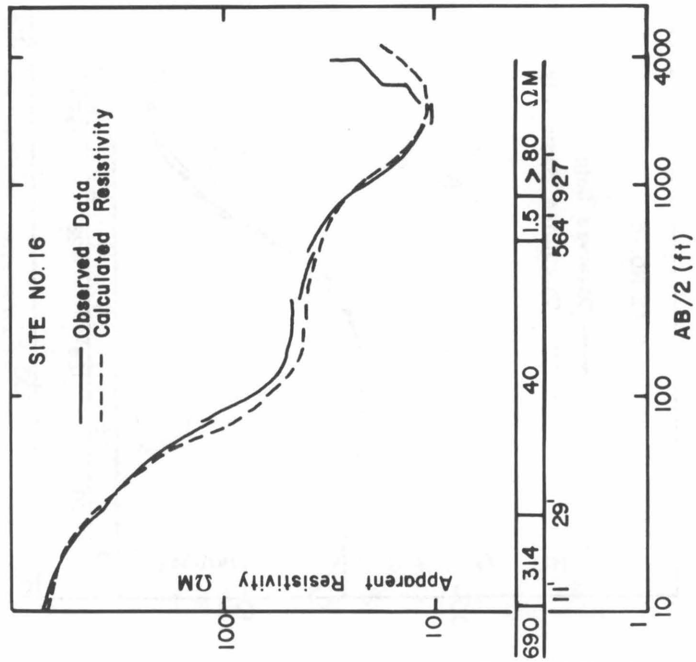
SITE NO. 16
Observed Data
Calculated Resistivity
Apparent Resistivity ΩM
100
10
1
10
100
1000
4000
AB/2 (ft)
690
314
40
1.5
>80 ΩM
11
29
564
927

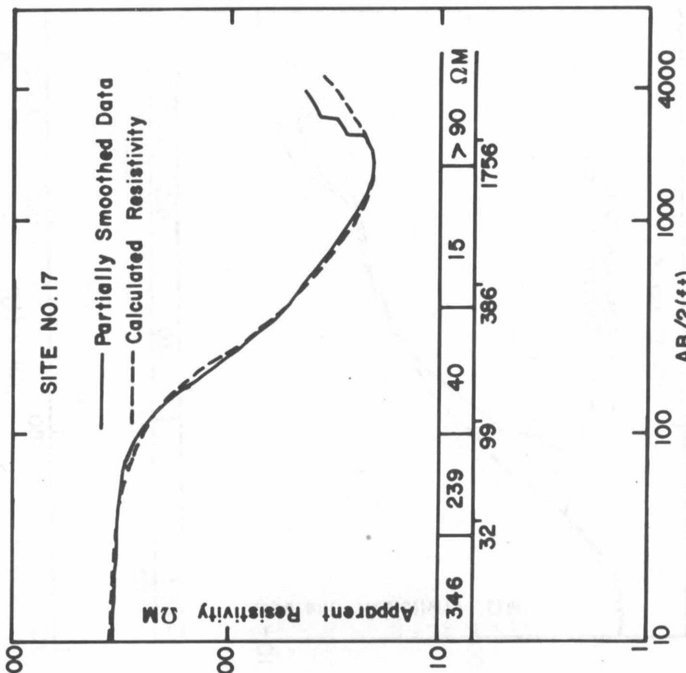
SITE NO. 17
Partially Smoothed Data
Calculated Resistivity
Apparent Resistivity ΩM
AB/2(ft)
1000
100
10
1
10
100
1000
4000
346
239
40
15
> 90 ΩM
32
99
386
1756

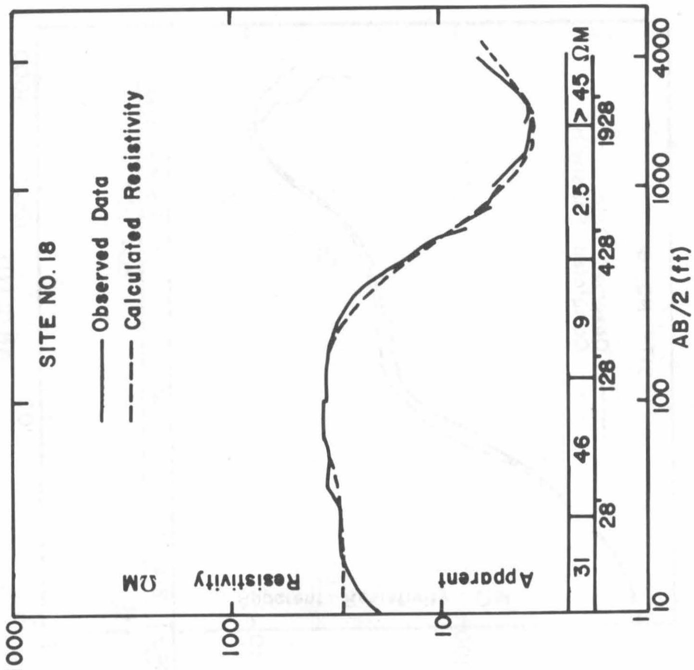
SITE NO. 18
Observed Data
Calculated Resistivity
Apparent Resistivity ΩM
AB/2 (ft)
1000
100
10
1
10
100
1000
4000
31
46
9
2.5
> 45 ΩM
28
128
428
1928

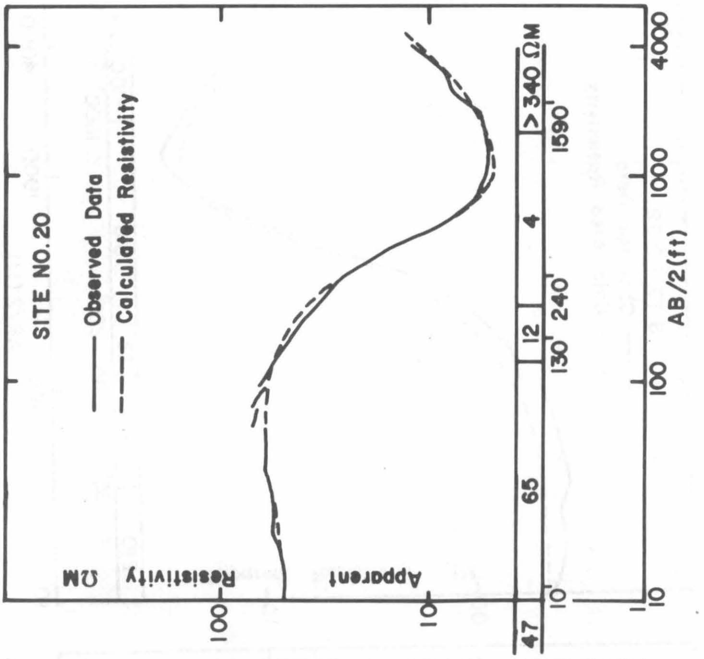
SITE NO. 20
Observed Data
Calculated Resistivity
Apparent Resistivity ΩM
100
10
1
10
100
1000
4000
AB/2 (ft)
47
65
12
4
> 340 ΩM
10
130
240
1590

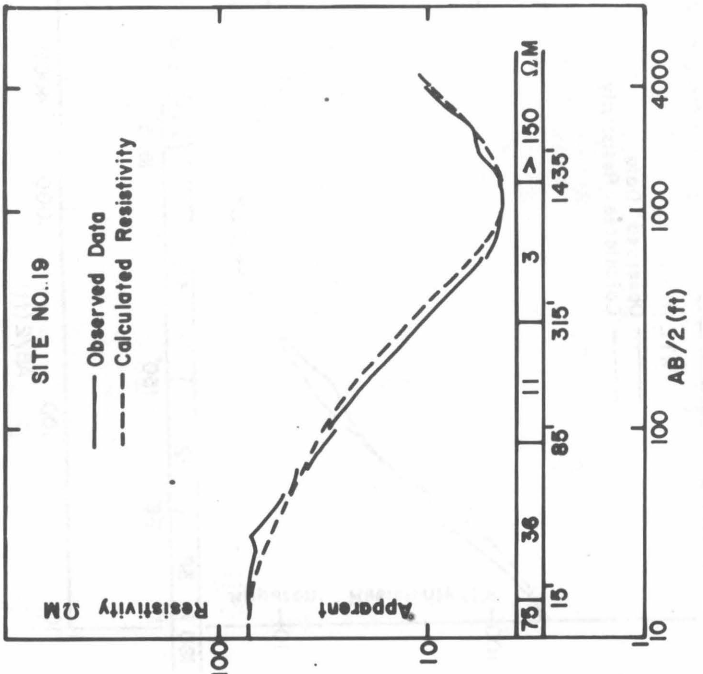
SITE NO. 19
Observed Data
Calculated Resistivity
Apparent Resistivity ΩM
100
10
1
10
100
1000
4000
AB/2 (ft)
75
36
11
3
> 150 ΩM
15
85
315
1435

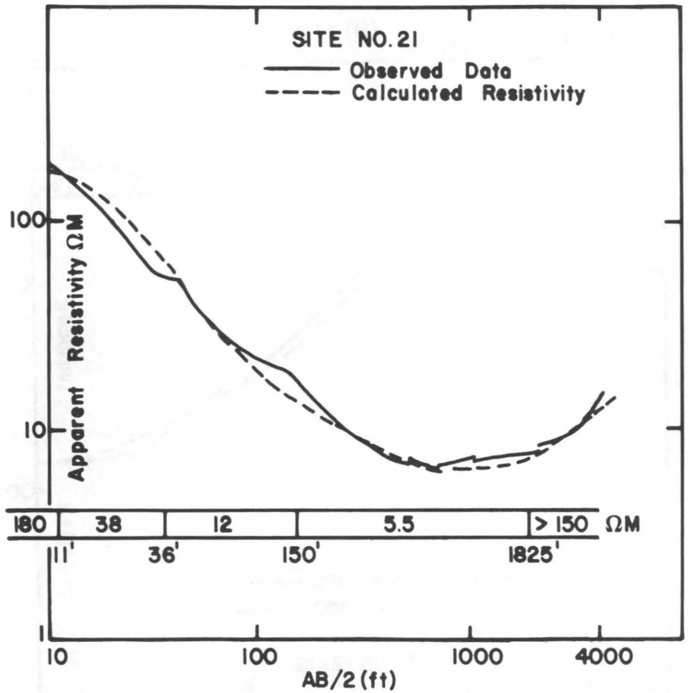
SITE NO. 21
Observed Data
Calculated Resistivity
Apparent Resistivity ΩM
100
10
1
180
38
12
5.5
> 150 ΩM
11'
36'
150'
1825'
10
100
1000
4000
AB/2 (ft)

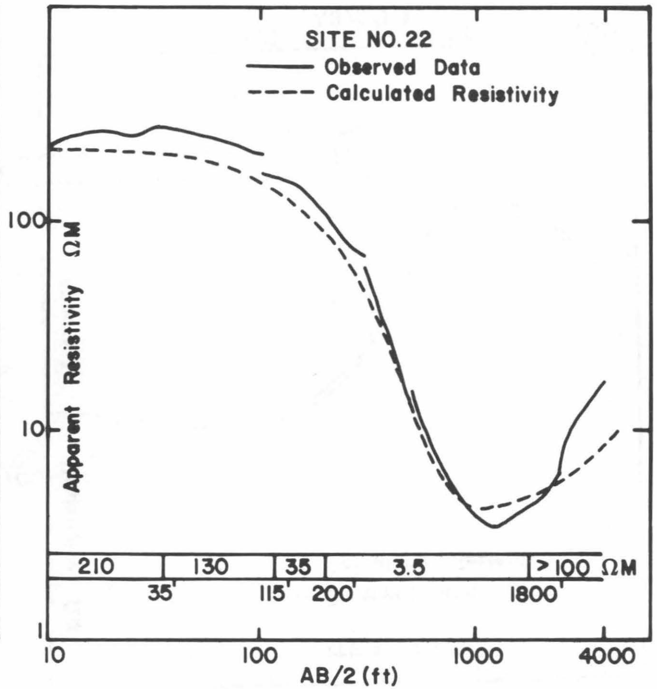
SITE NO. 22
Observed Data
Calculated Resistivity
Apparent Resistivity ΩM
100
10
1
210
130
35
3.5
> 100 ΩM
35'
115'
200'
1800'
10
100
1000
4000
AB/2 (ft)

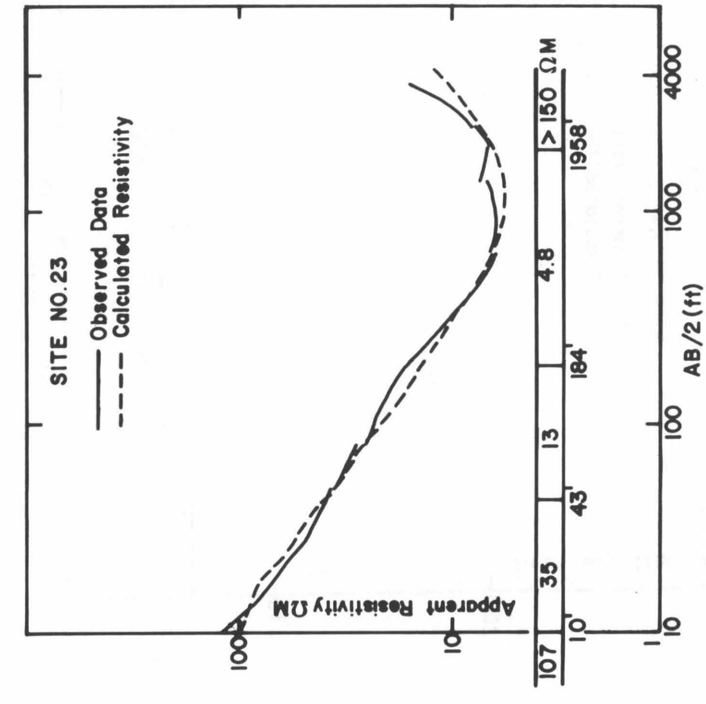

SITE NO.23
Observed Data
Calculated Resistivity
Apparent Resistivity ΩM
100
10
10
100
1000
4000
AB/2 (ft)
107
10
35
43
13
184
4.8
1958
> 150 ΩM

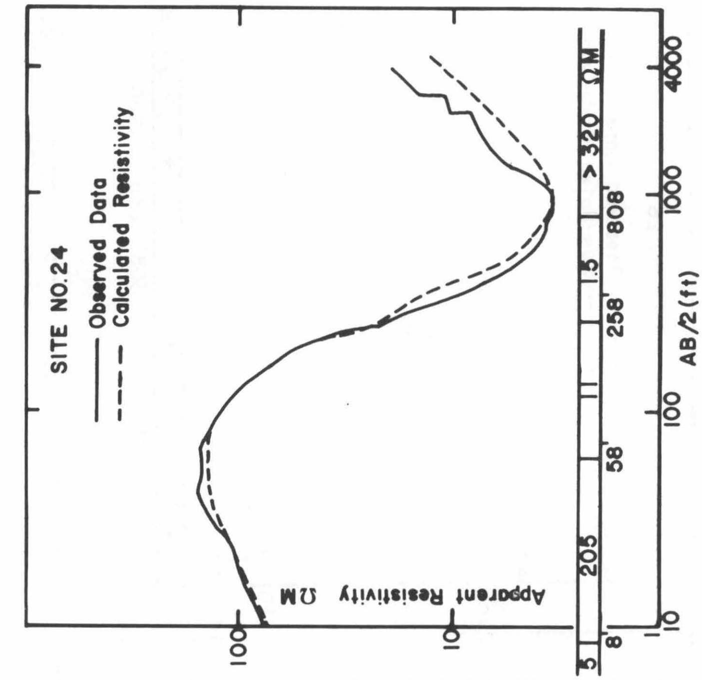

SITE NO.24
Observed Data
Calculated Resistivity
Apparent Resistivity ΩM
100
10
10
100
1000
4000
AB/2 (ft)
5
8
205
58
258
1.5
808
> 320 ΩM

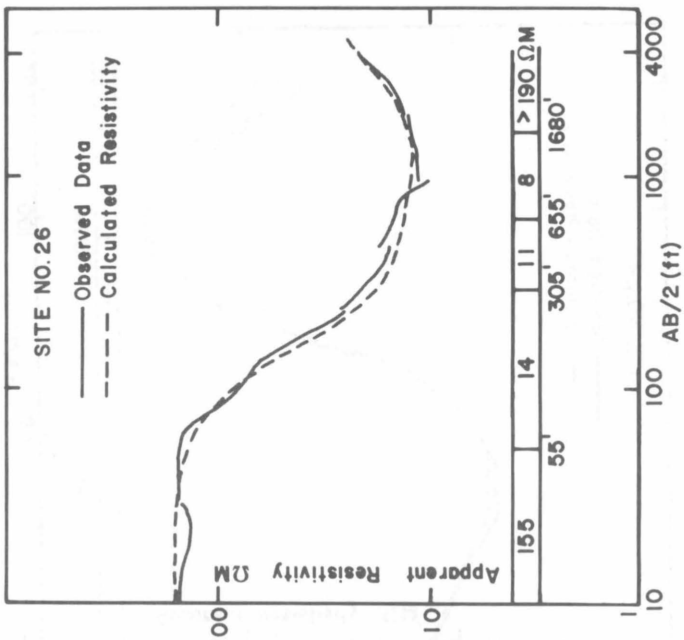
SITE NO. 26
Observed Data
Calculated Resistivity
Apparent Resistivity ΩM
100
10
1
10
100
1000
4000
AB/2 (ft)
155
55
14
305'
11
655'
8
1680'
>190 ΩM

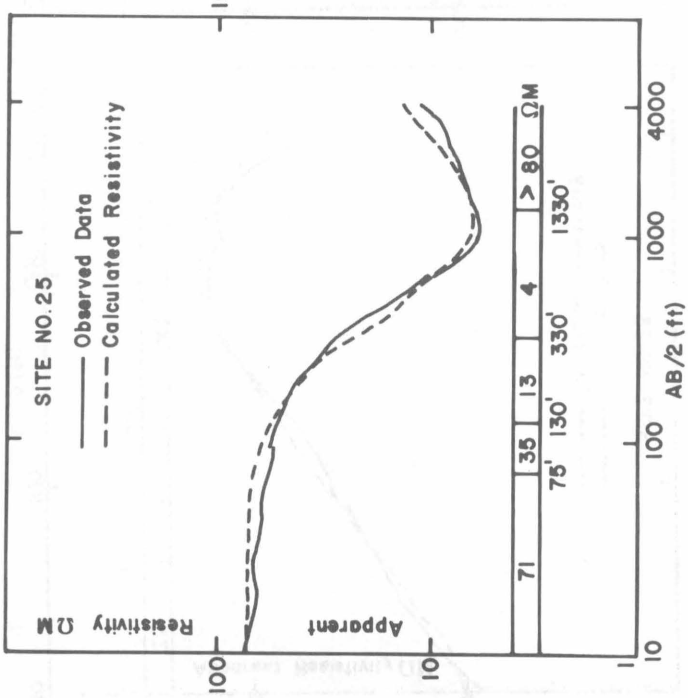
SITE NO. 25
Observed Data
Calculated Resistivity
Apparent Resistivity ΩM
100
10
1
10
100
1000
4000
AB/2 (ft)
71
75'
35
130'
13
330'
4
1330'
>80 ΩM

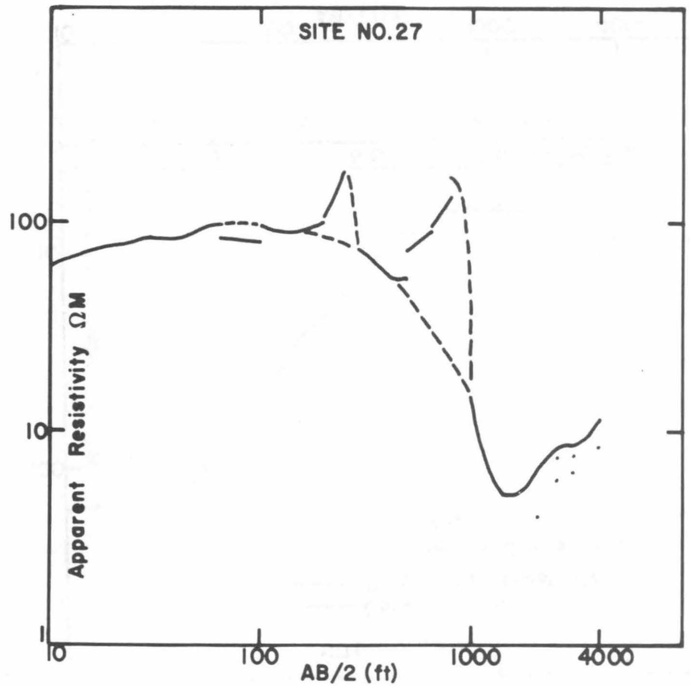
SITE NO.27
Apparent Resistivity ΩM
100
10
1
10
100
1000
4000
AB/2 (ft)

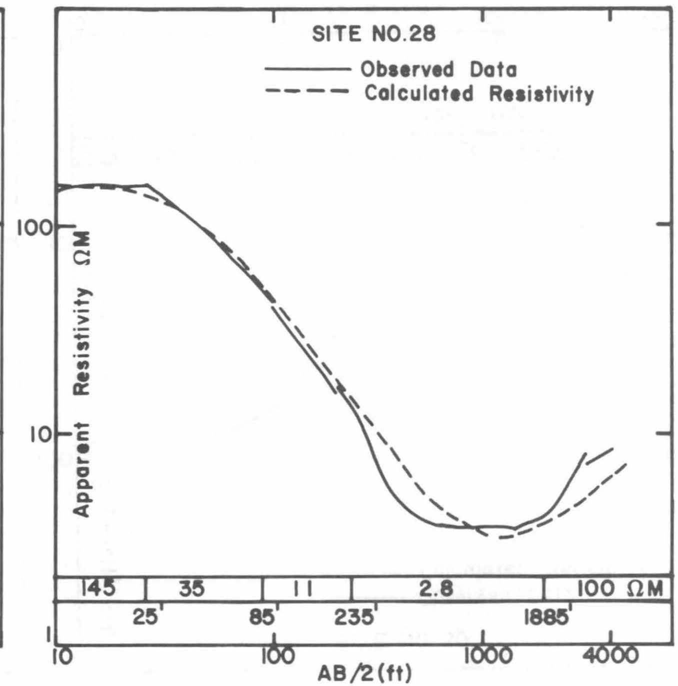
SITE NO.28
Observed Data
Calculated Resistivity
Apparent Resistivity ΩM
100
10
1
145
35
11
2.8
100 ΩM
25'
85'
235'
1885'
10
100
1000
4000
AB/2 (ft)

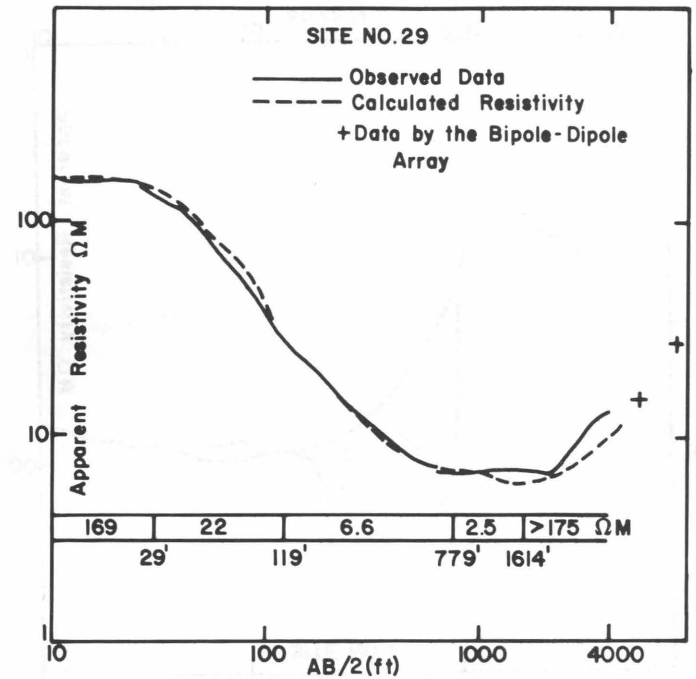
SITE NO. 29
Observed Data
Calculated Resistivity
+Data by the Bipole-Dipole Array
Apparent Resistivity ΩM
100
10
1
169
22
6.6
2.5
>175 ΩM
29'
119'
779'
1614'
10
100
1000
4000
AB/2(ft)

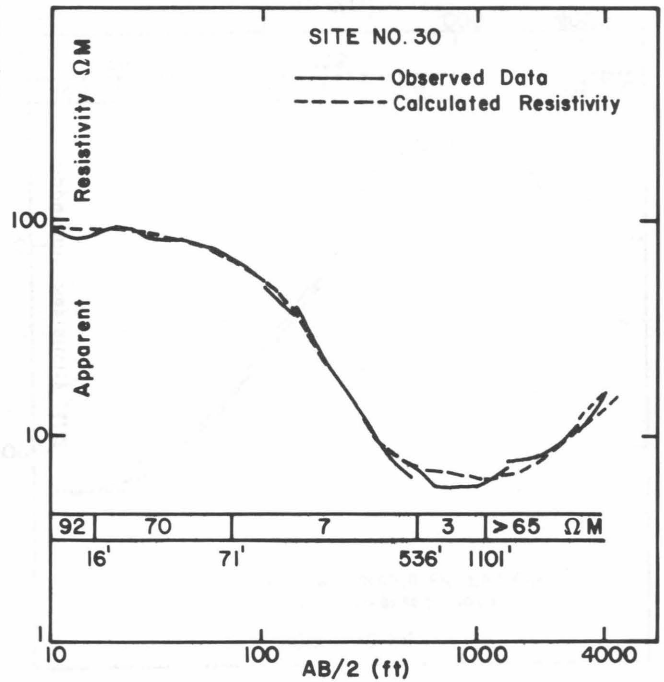
SITE NO. 30
Observed Data
Calculated Resistivity
Apparent Resistivity ΩM
100
10
1
92
70
7
3
>65 ΩM
16'
71'
536'
1101'
10
100
1000
4000
AB/2 (ft)

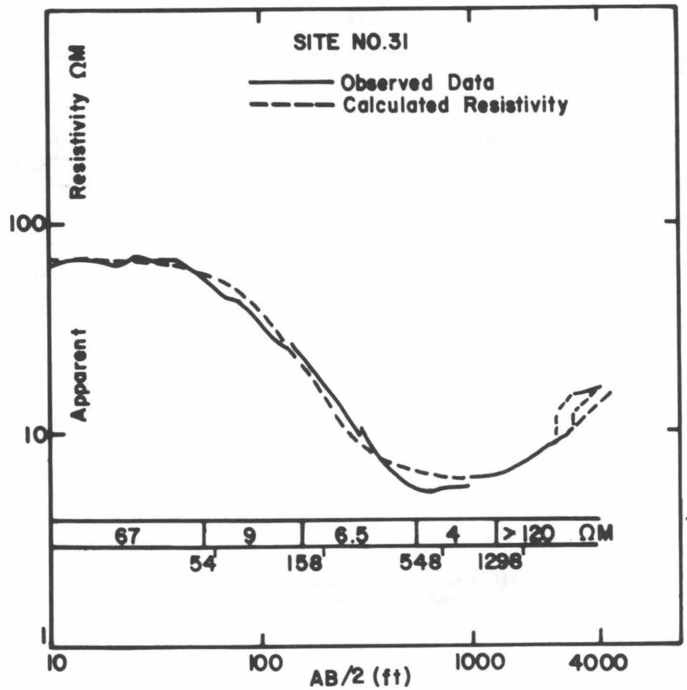
SITE NO.31
Observed Data
Calculated Resistivity
Apparent Resistivity ΩM
100
10
1
67
9
6.5
4
> 120
ΩM
54
158
548
1298
10
100
1000
4000
AB/2 (ft)

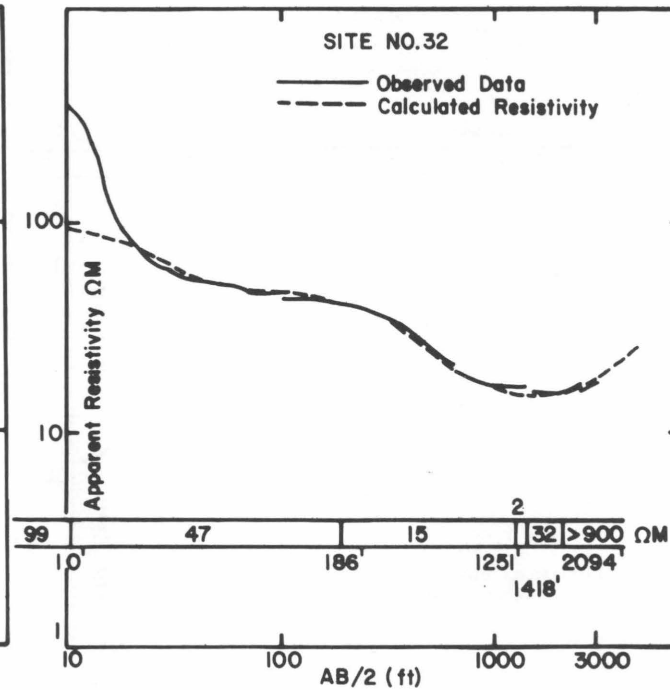
SITE NO.32
Observed Data
Calculated Resistivity
Apparent Resistivity ΩM
100
10
1
99
47
15
2
32
>900
ΩM
10
186
1251
1418'
2094
10
100
1000
3000
AB/2 (ft)

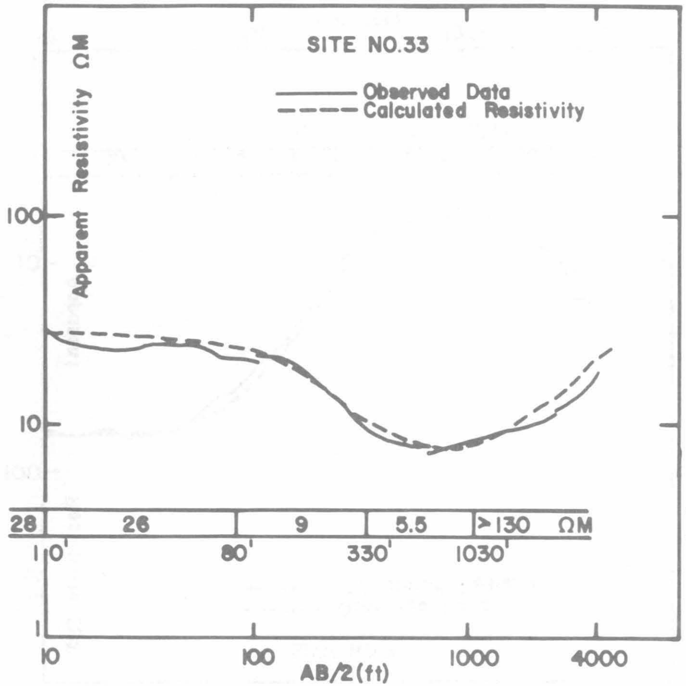
SITE NO.33
Observed Data
Calculated Resistivity
Apparent Resistivity ΩM
100
10
1
28
26
9
5.5
>130
ΩM
10'
80'
330'
1030'
10
100
1000
4000
AB/2(ft)

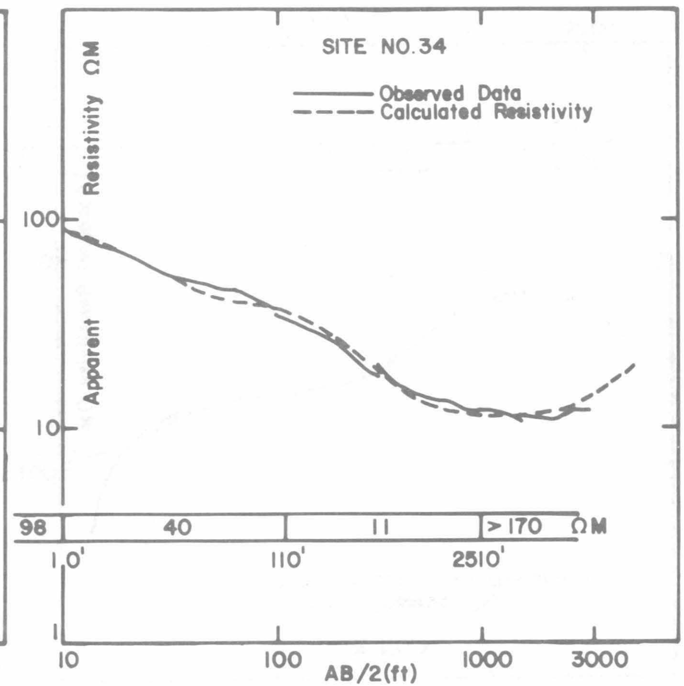
SITE NO.34
Observed Data
Calculated Resistivity
Apparent Resistivity ΩM
100
10
1
98
40
11
>170
ΩM
1.0'
110'
2510'
10
100
1000
3000
AB/2(ft)

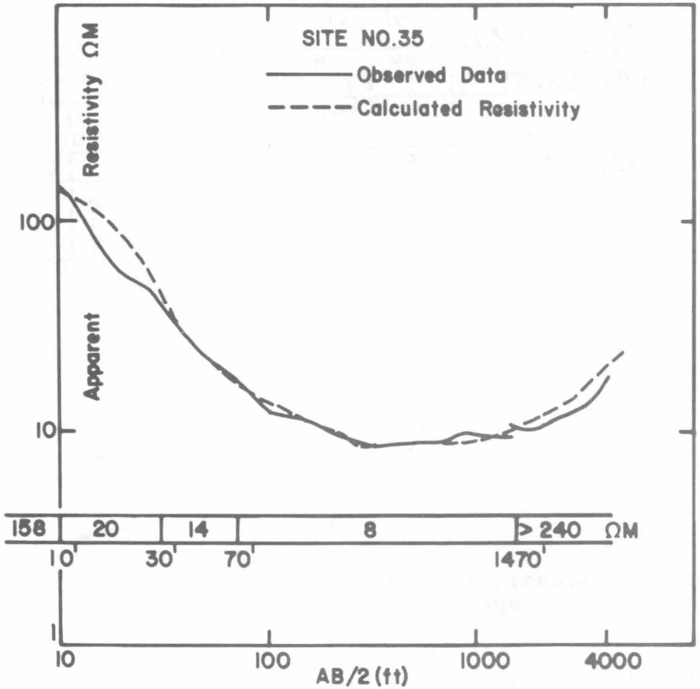

SITE NO.35
Observed Data
Calculated Resistivity
Apparent Resistivity ΩM
100
10
1
158
20
14
8
> 240 ΩM
10
30
70
1470
10
100
1000
4000
AB/2 (ft)

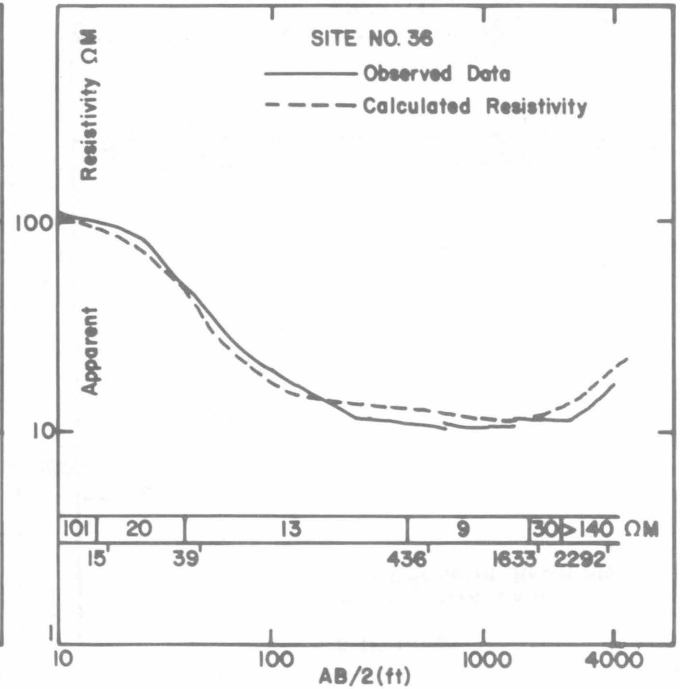

SITE NO. 36
Observed Data
Calculated Resistivity
Apparent Resistivity ΩM
100
10
1
101
20
13
9
30
>140 ΩM
15
39
436
1633
2292
10
100
1000
4000
AB/2 (ft)

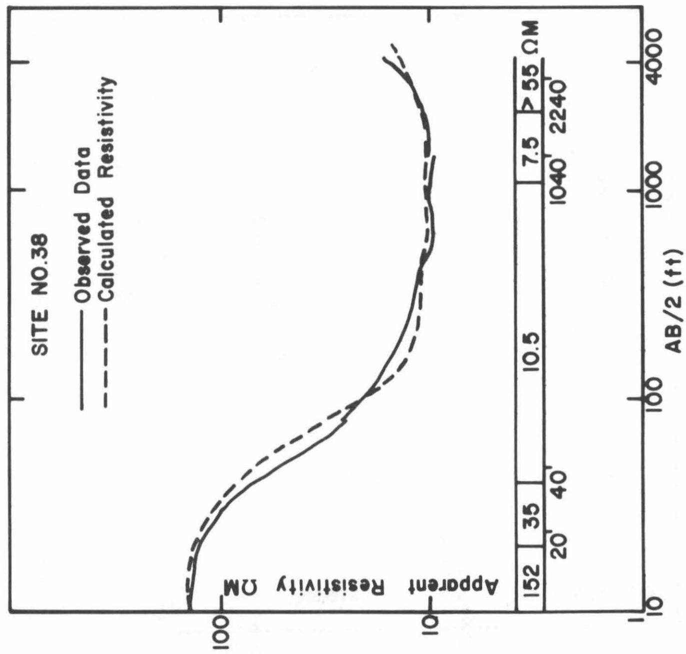
SITE NO.38
Observed Data
Calculated Resistivity
Apparent Resisitivity ΩM
100
10
1
10
100
1000
4000
AB/2 (ft)
152
35
10.5
7.5
> 55 ΩM
20
40
1040
2240

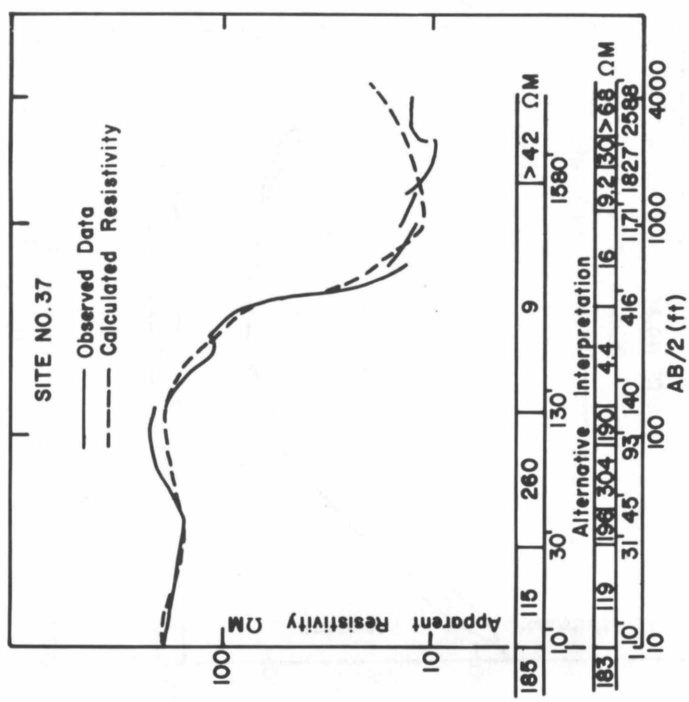
SITE NO.37
Observed Data
Calculated Resistivity
Apparent Resisitivity ΩM
100
10
1
10
100
1000
4000
AB/2 (ft)
185
115
260
9
> 42 ΩM
10
30
130
1580
Alternative Interpretation
183
119
196
304
190
4.4
16
9.2
130
> 68 ΩM
10
31
45
93
140
416
1171
1827
2588

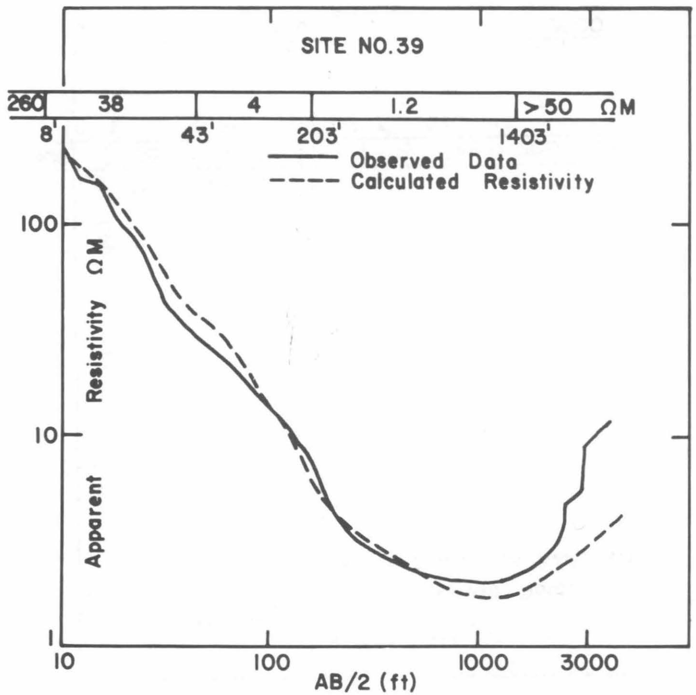

SITE NO.39
260
38
4
1.2
>50 ΩM
8'
43'
203'
1403'
Observed Data
Calculated Resistivity
Apparent Resistivity ΩM
1
10
100
10
100
1000
3000
AB/2 (ft)

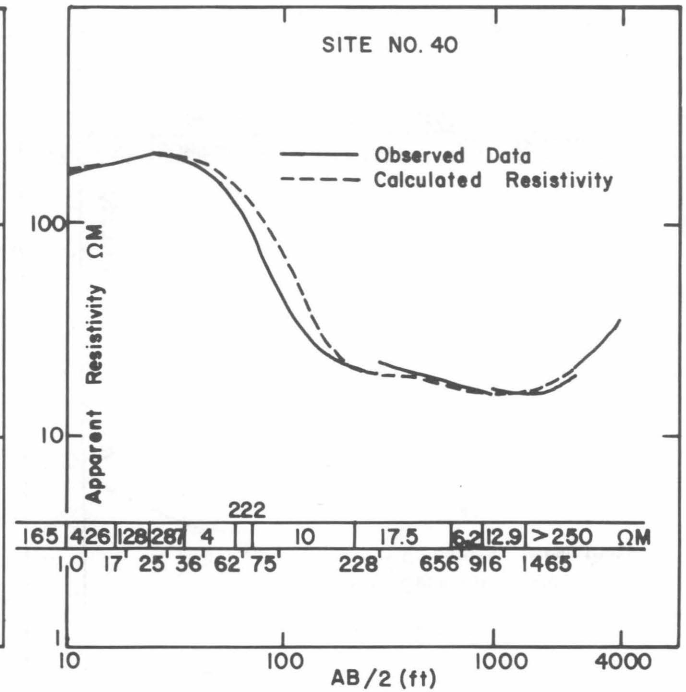

SITE NO. 40
Observed Data
Calculated Resistivity
Apparent Resistivity ΩM
222
165
426
128
287
4
10
17.5
6.2
12.9
>250 ΩM
1.0
17
25
36
62
75
228
656
916
1465
1
10
100
10
100
1000
4000
AB/2 (ft)

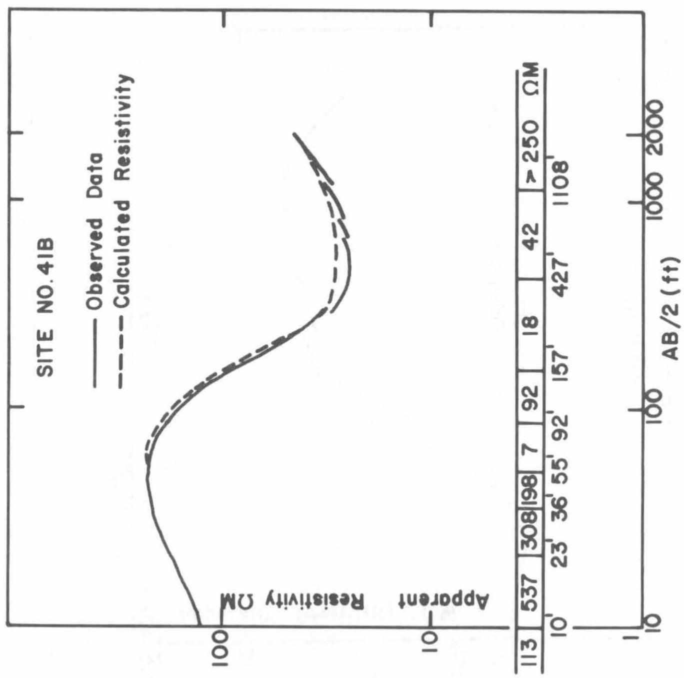
SITE NO. 41B
Observed Data
Calculated Resistivity
Apparent Resistivity ΩM
AB/2 (ft)
113 | 537 | 308 | 198 | 7 | 92 | 18 | 42 | > 250 ΩM
10 23 36 55 92 157 427 1108
1 10 100 1000 2000
10 100

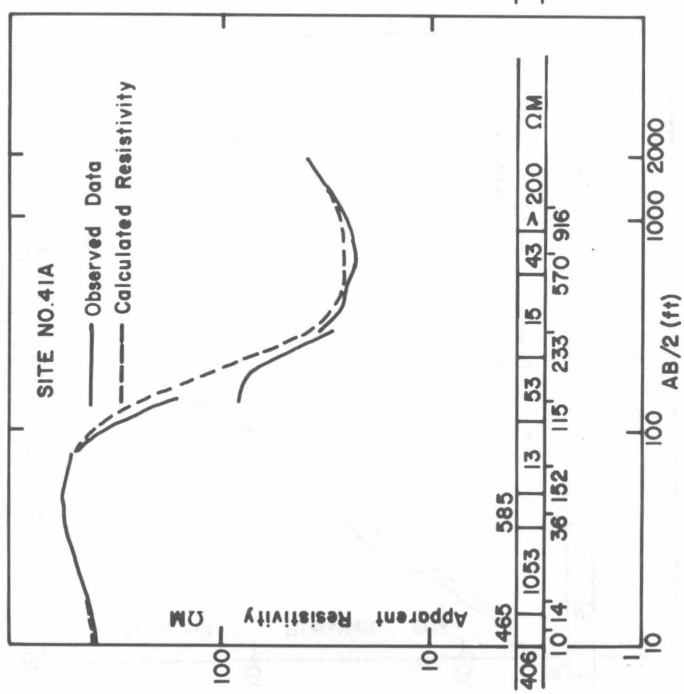
SITE NO. 41A
Observed Data
Calculated Resistivity
Apparent Resistivity ΩM
AB/2 (ft)
406 | 465 | 1053 | 585 | 13 | 53 | 15 | 43 | > 200 ΩM
10 14 36 152 115 233 570 916
1 10 100 1000 2000
10 100

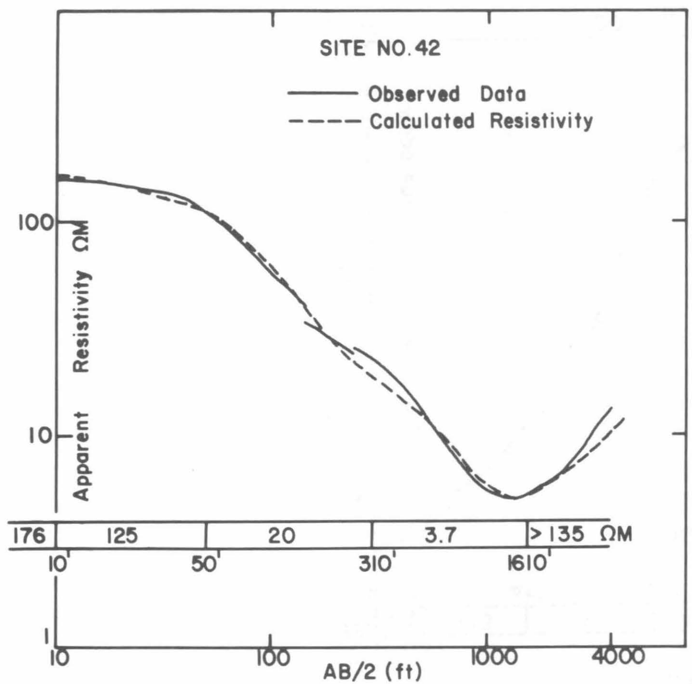
SITE NO. 42
Observed Data
Calculated Resistivity
Apparent Resistivity ΩM
100
10
1
176
125
20
3.7
> 135 ΩM
10'
50'
310'
1610'
10
100
1000
4000
AB/2 (ft)

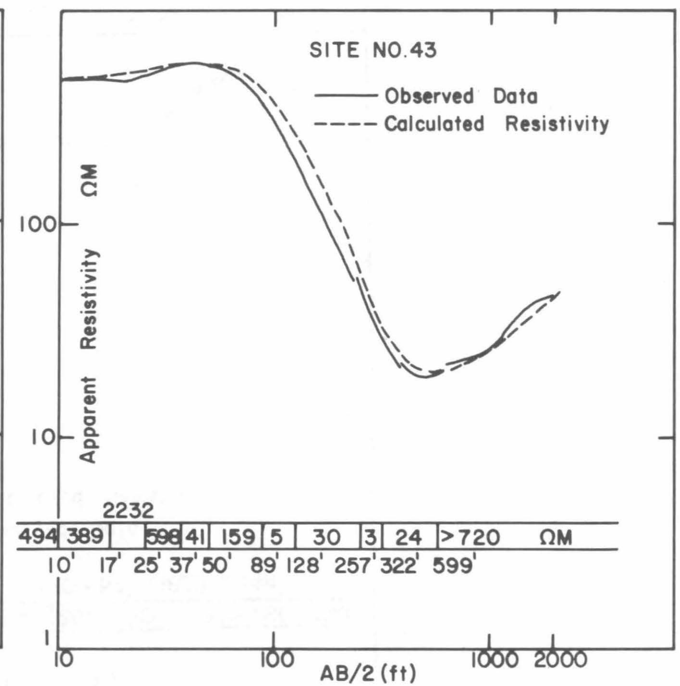
SITE NO. 43
Observed Data
Calculated Resistivity
Apparent Resistivity ΩM
100
10
1
2232
494
389
598
41
159
5
30
3
24
>720
ΩM
10'
17'
25'
37'
50'
89'
128'
257'
322'
599'
10
100
1000
2000
AB/2 (ft)

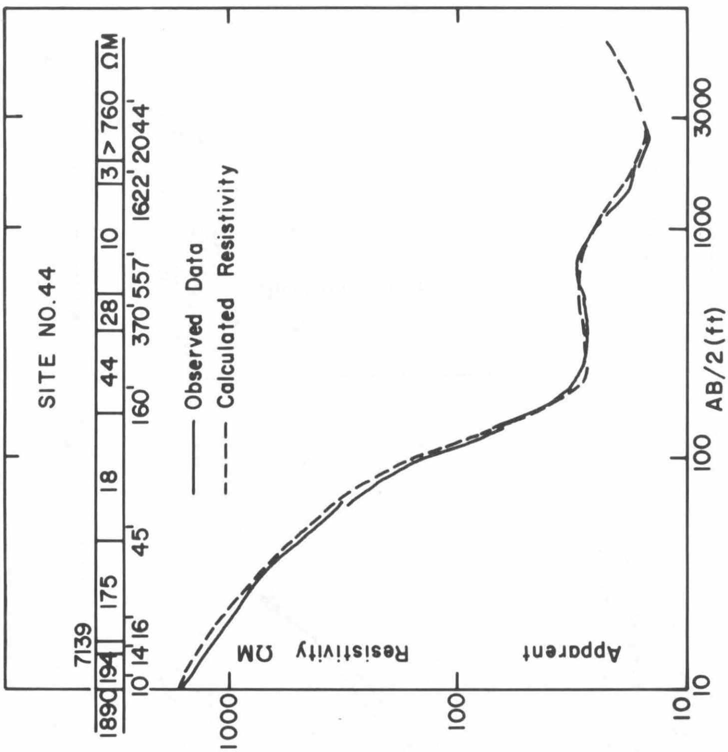
SITE NO.44
1890
7139
194
175
18
44
28
10
3
> 760 ΩM
10' 14' 16' 45' 160' 370' 557' 1622' 2044'
Observed Data
Calculated Resistivity
Apparent Resistivity ΩM
1000
100
10
10
100
1000
3000
AB/2 (ft)

FIGURES

Figure 1

Location Map of Resistivity Soundings

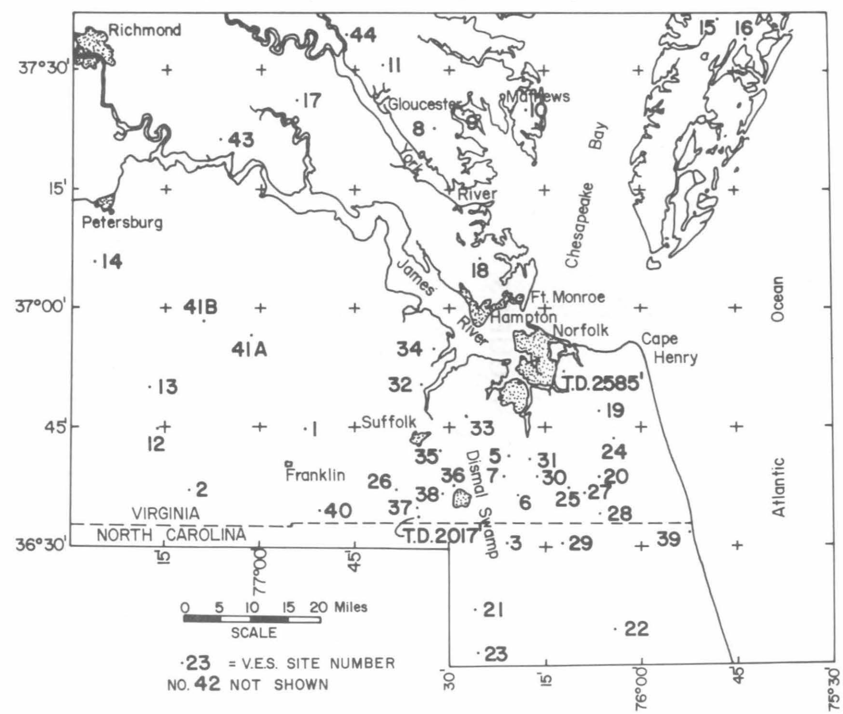

Figure 2

Major Morphologic Features of the Coastal Plain Region
(after Oaks and Coch, 1973)

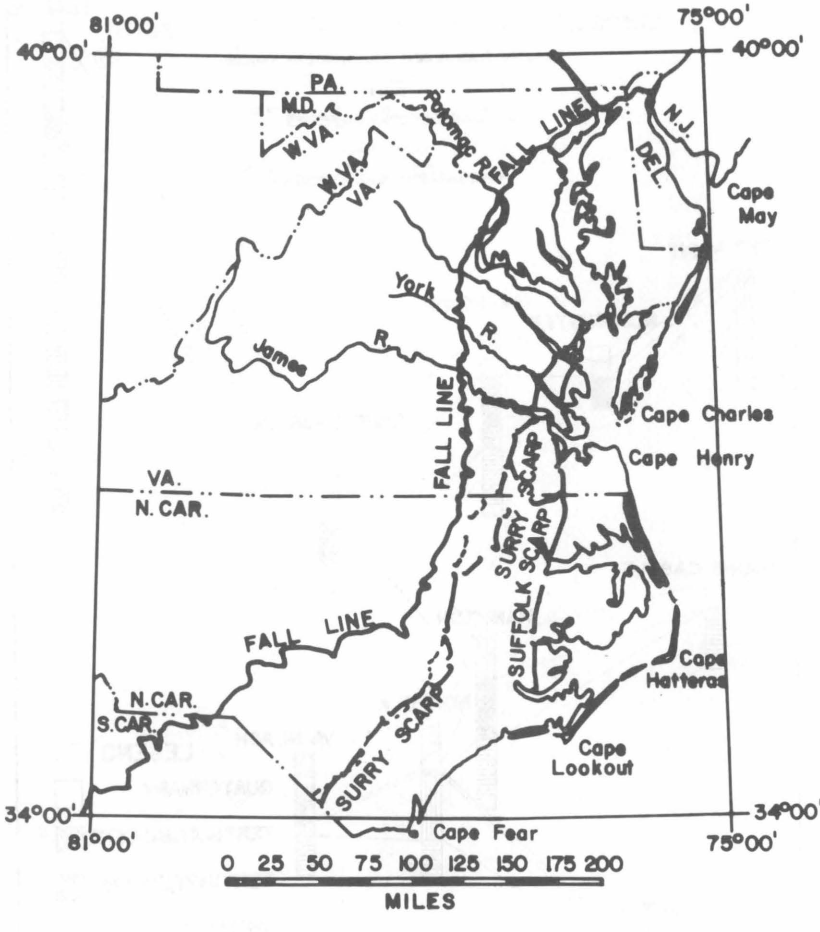

Figure 3

Correlation of Time-Stratigraphic Units,
Coastal Plain Region, Southeastern Virginia

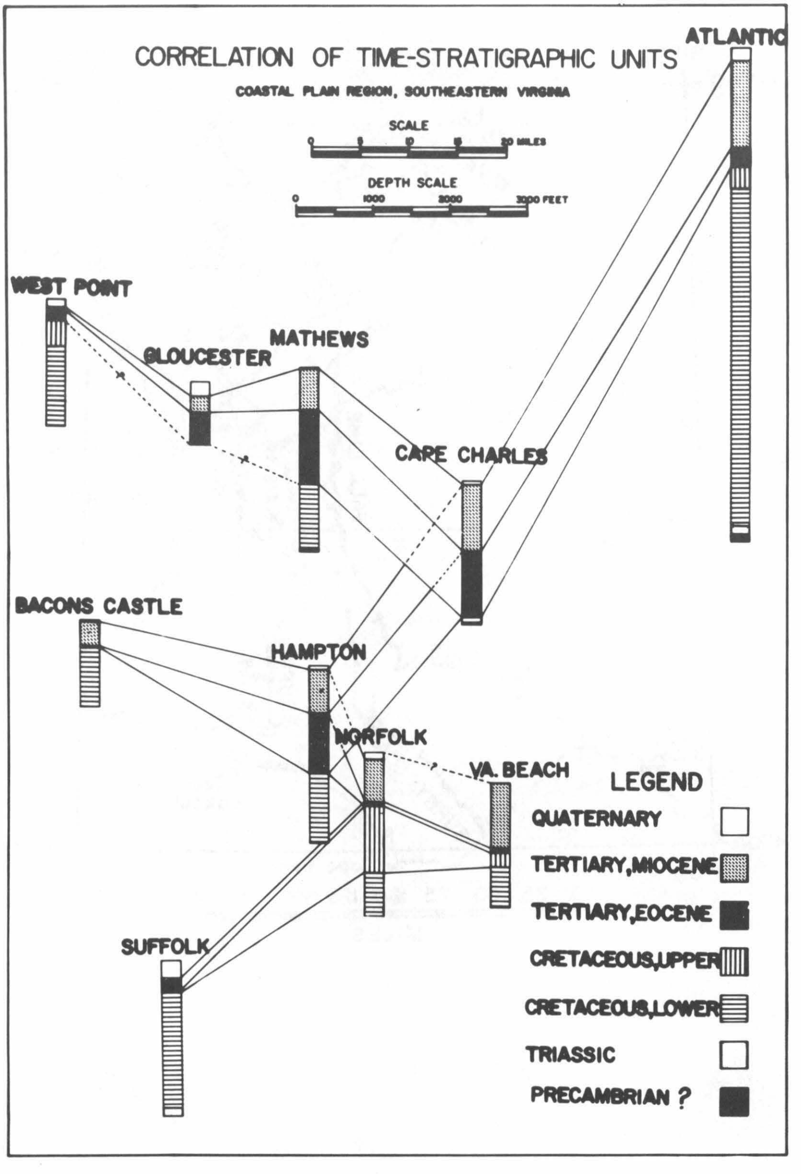

Figure 4

Columnar Section of the Coastal Plain Sediments
Giving Water-Bearing Properties of Formations

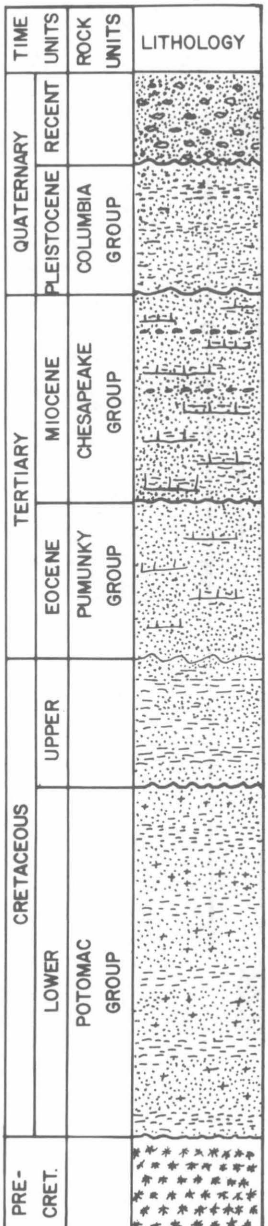

Sands and gravels. Exposed along beaches in the Norfolk area. Attains a thickness of 140 ft. at Cape Henry. Yields small quantities of water.

Sands and clays of continental origin to the west and of marine origin to the east. Thickness ranges between 0 and 600 ft. The sands are excellent aquifers.

Shell beds, marls, dark blue and grey clays and sands, of marine origin. Thickness ranges between 0 and 700 ft. To the west of Norfolk, the Yorktown becomes an important water-bearing formation.

Glauconitic sands and marls of marine origin. Thickness ranges between 0 and 700 ft. Not an important source of water.

Interbedded sands and clays of near-shore marine origin. Thickness ranges between 0 and 200 ft. The sands yield small quantities of water.

Interbedded arkosic sands and clays of continental origin. Individual strata generally lenticular. Thickness ranges between 0 and 1000 ft. In the Eastern Shore Area, about 4300 ft. were encountered. Exposed near the Fall Zone. Found in wells at Norfolk and vicinity. The sands are excellent sources of water. To the east of the Dismal Swamp, the water is brackish.

Mostly igneous and metamorphic rocks. In some wells, Jurassic sands and clays were encountered. Some wells near the Fall Zone produce excellent water from granites.

Figure 5

The Schlumberger Array

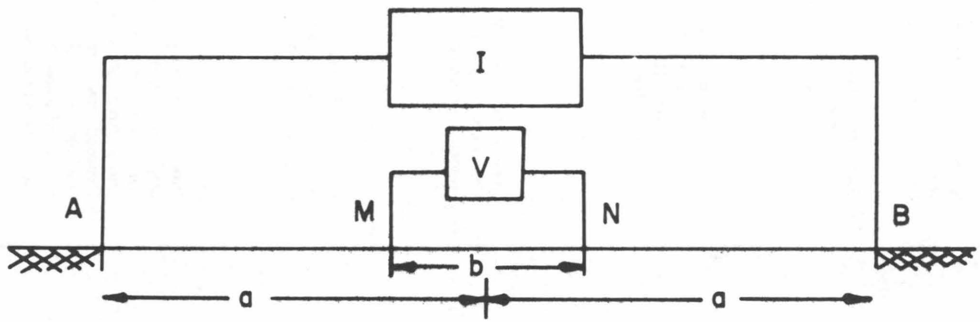

Figure 6

A Layered-Earth Model and
Its One Layer Equivalents

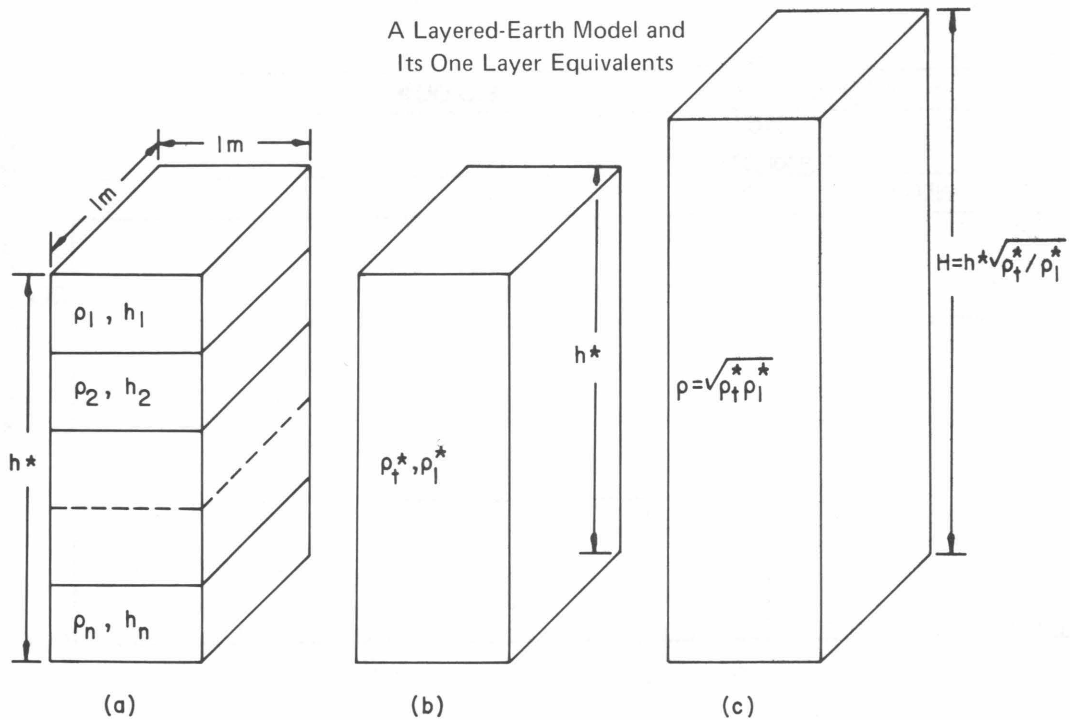

Figure 7

Illustration of the Principle of Equivalence

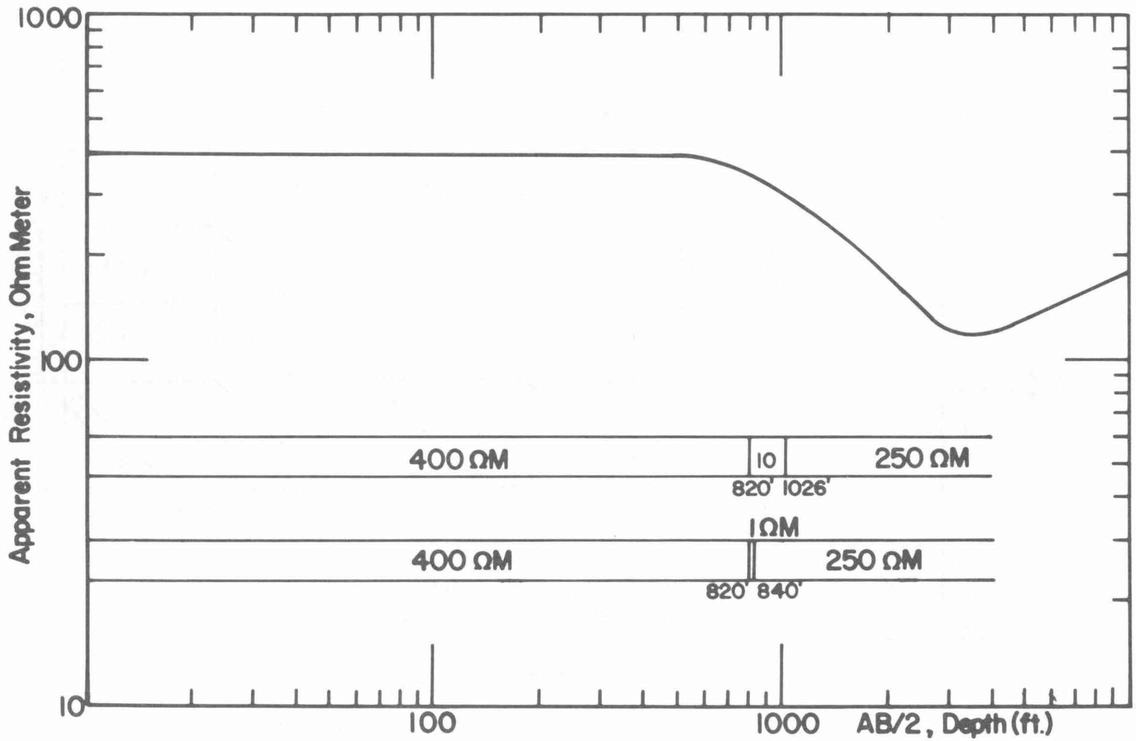

Figure 8

Illustration of the Principle of Suppression
(modified from Kunetz, 1966)

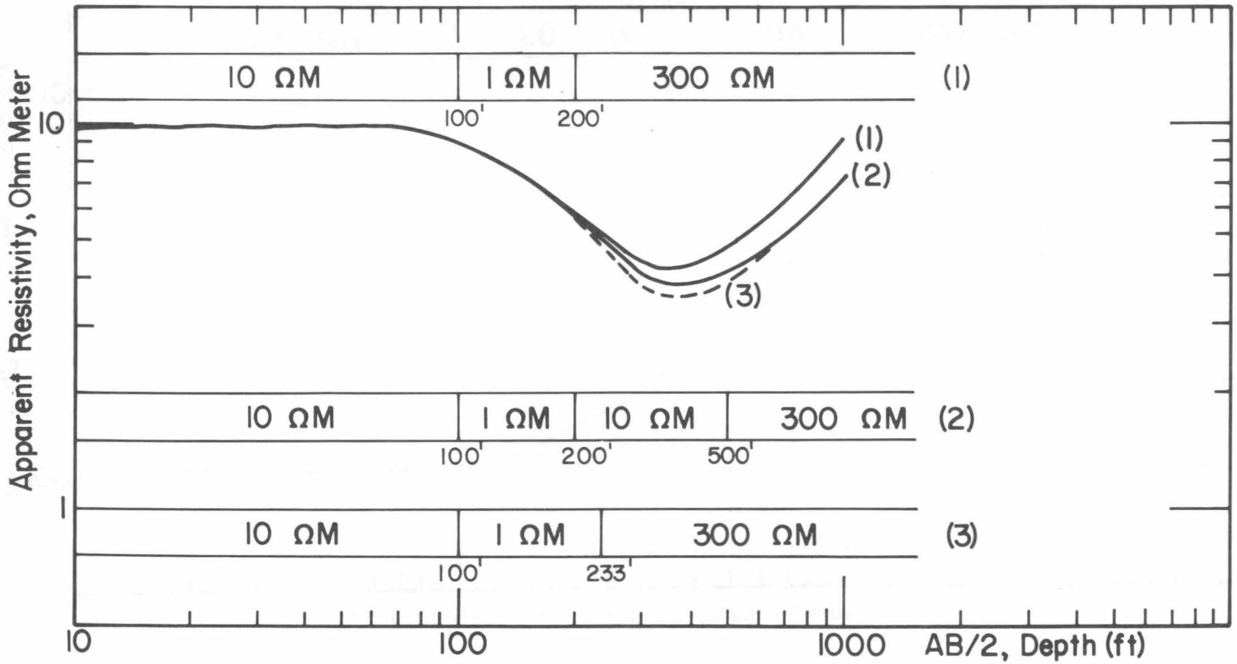

Figure 9

Two Possible Interpretations of the "Electric Basement"

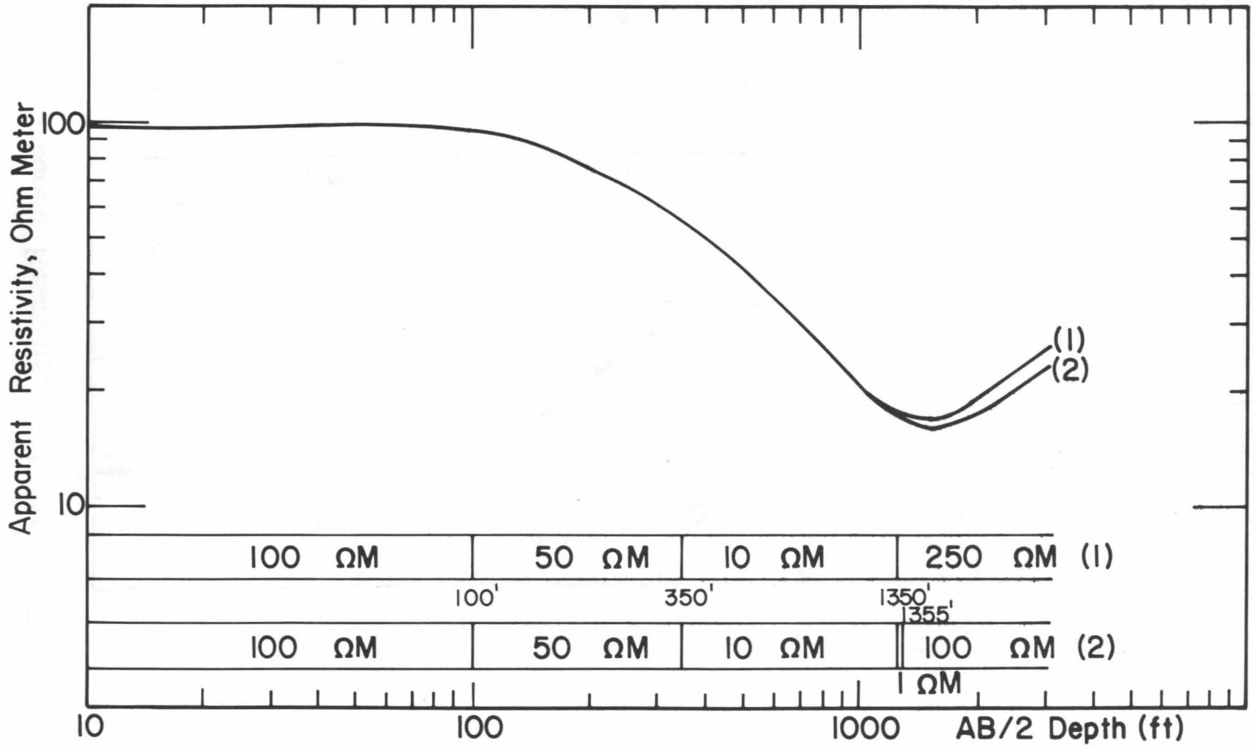

Figure 10

The Effect of Changes in Facies on the Shape of the Sounding Curve
(modified from Kunetz, 1966)

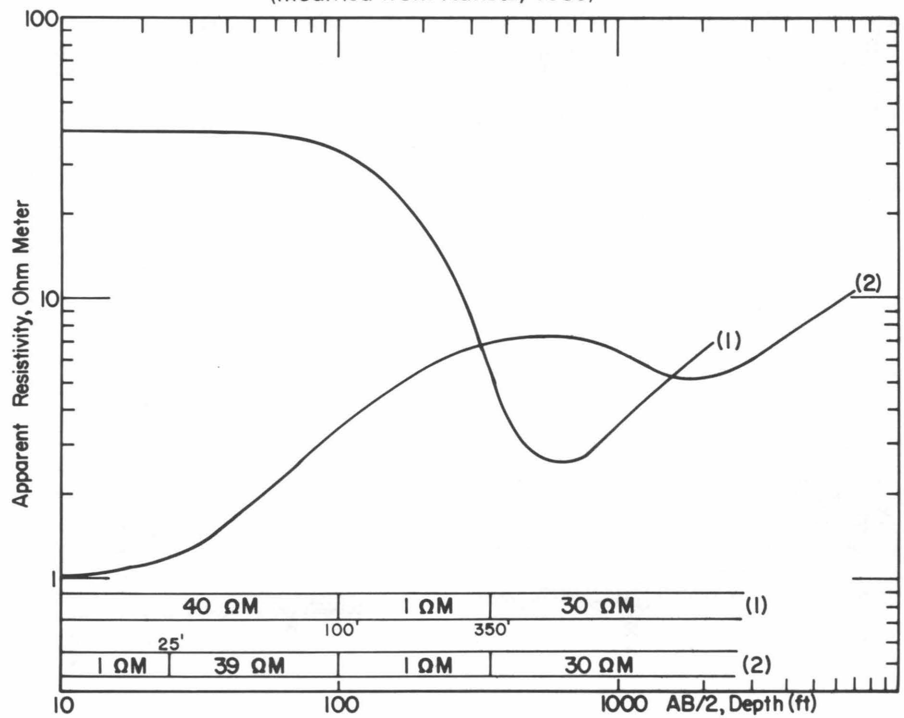

Figure 11

Correlation Between Resistivity Well-Logs
and VES Interpretations
(Note logarithmic (VES)and linear (16 inch normal) scales)

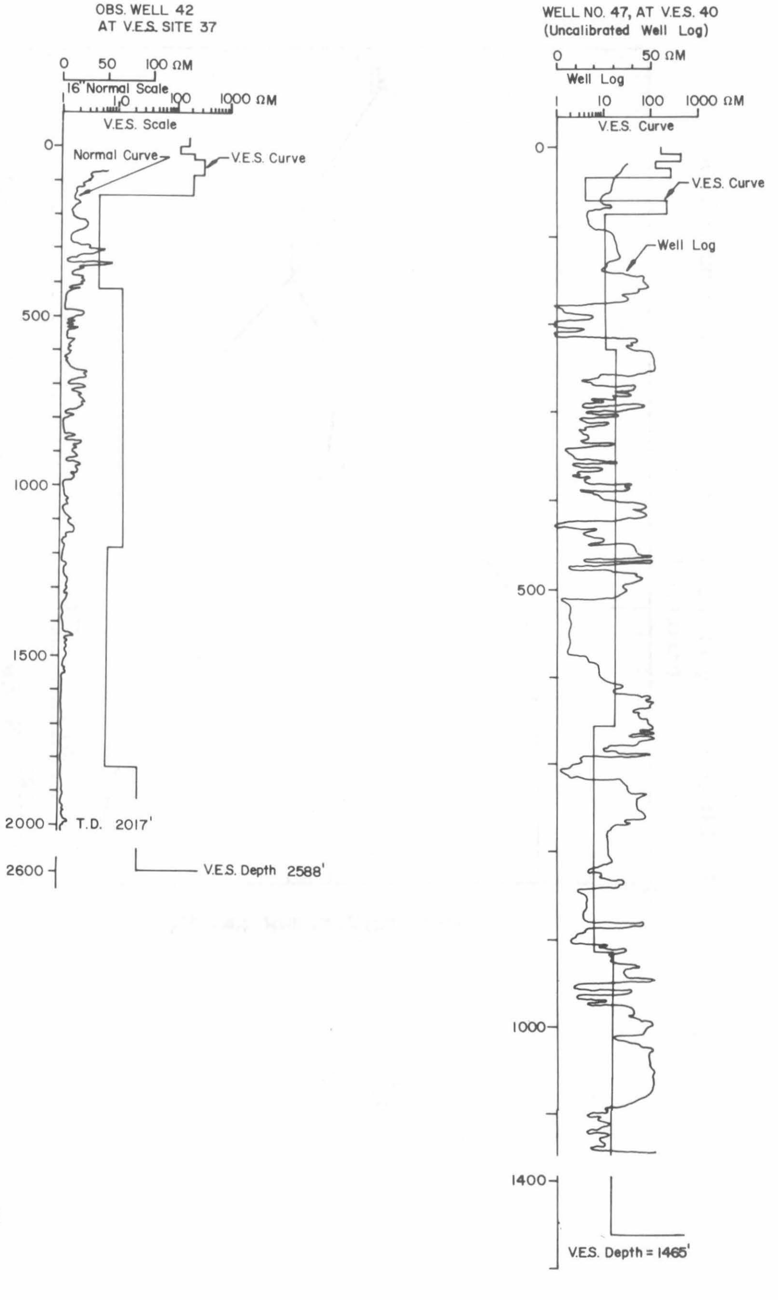

Figure 11
(Continued)

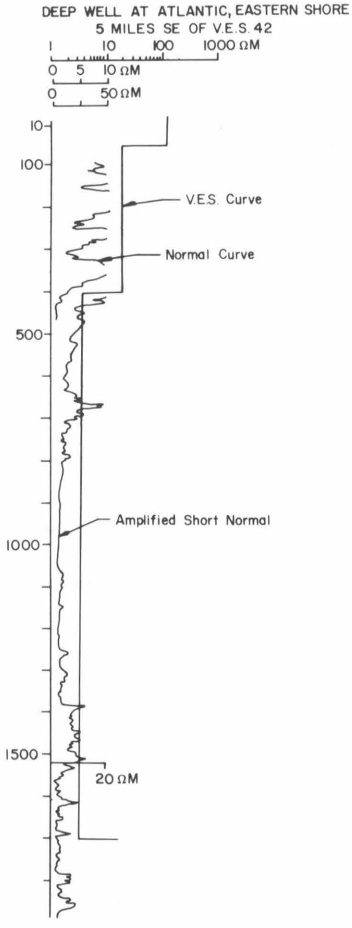

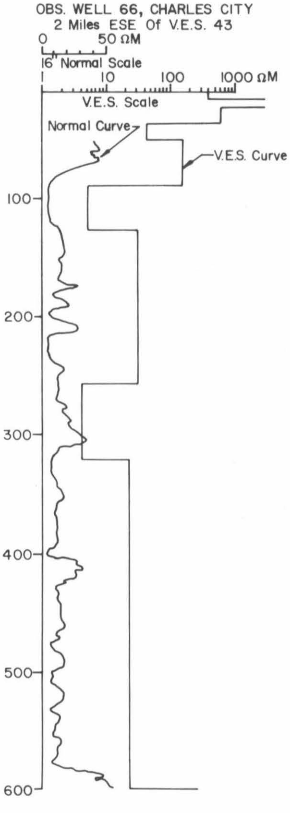

Figure 12

Transformation of VES Curve to DPS Curve (after Zohdy, 1972)

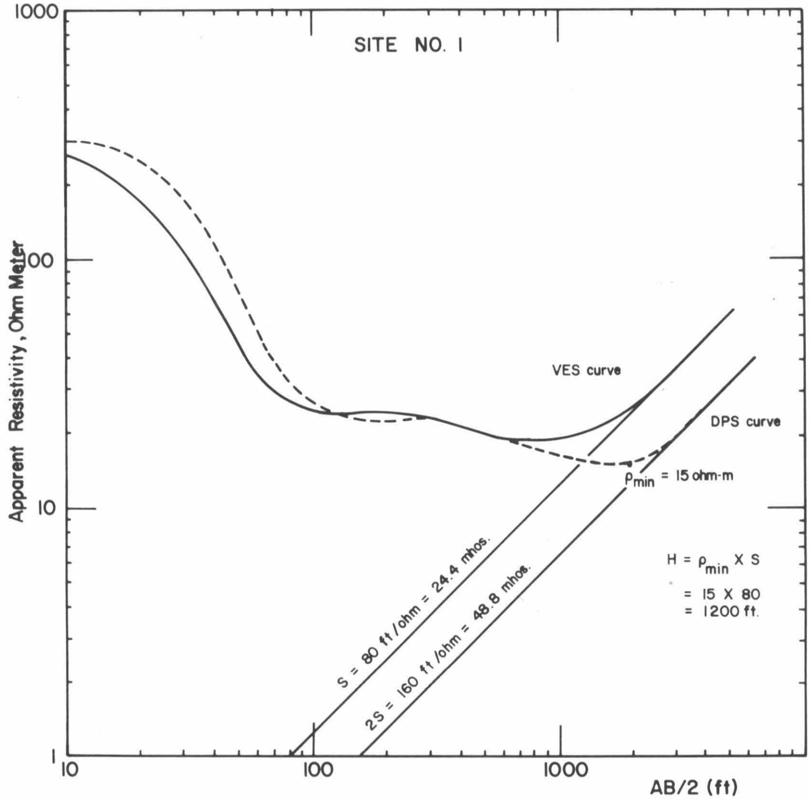

VIRGINIA WATER RESOURCES RESEARCH CENTER
BLACKSBURG, VIRGINIA 24061